Thunderstorm Generation by Bores and Solitons

Dr. Steve Koch

Director, National Severe Storms Laboratory

Bores as a Nocturnal CI Mechanism

- Bores and solitons were a frequent surprise event during IHOP (Knupp 2006: Koch et al. 2008; Parsons 2008)
- Radar observed 20 bore events on 15 different days between 2030 and 0500 CST (Wilson and Roberts 2006)
- However, only 6 of the 20 bores initiated thunderstorms
- What do we currently understand about why only some bores can produce Convection Initiation?
  - First, some basics about bore generation, dynamics, ducting
  - Then, a quick look at 3 case studies – one with explosive CI, another with no CI, and the third with localized CI – to try to understand some of the factors

Gravity Currents in Geophysical Flows

A gravity current is a horizontal mass flow driven by its greater density relative to its environment.

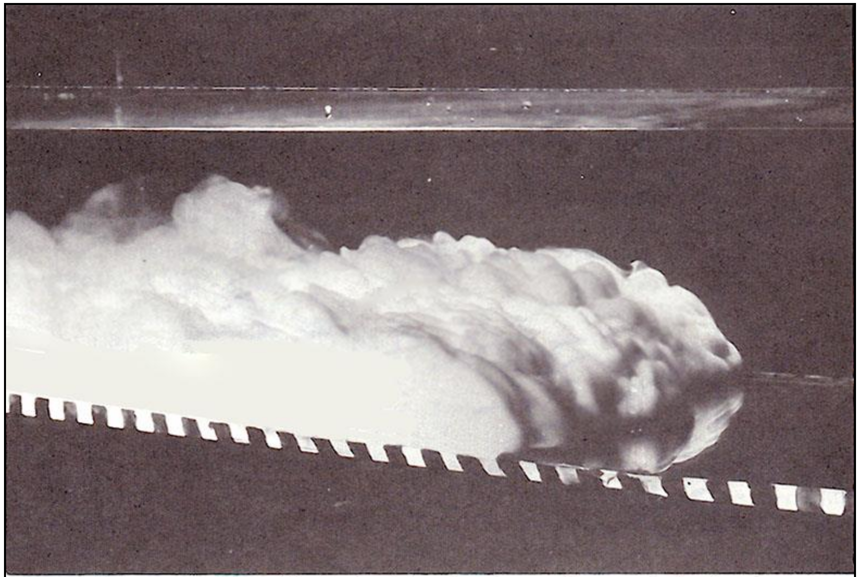

Lobes and clefts within the frontal region of a gravity current of salt water along the floor of a freshwater tank (Simpson 1987)

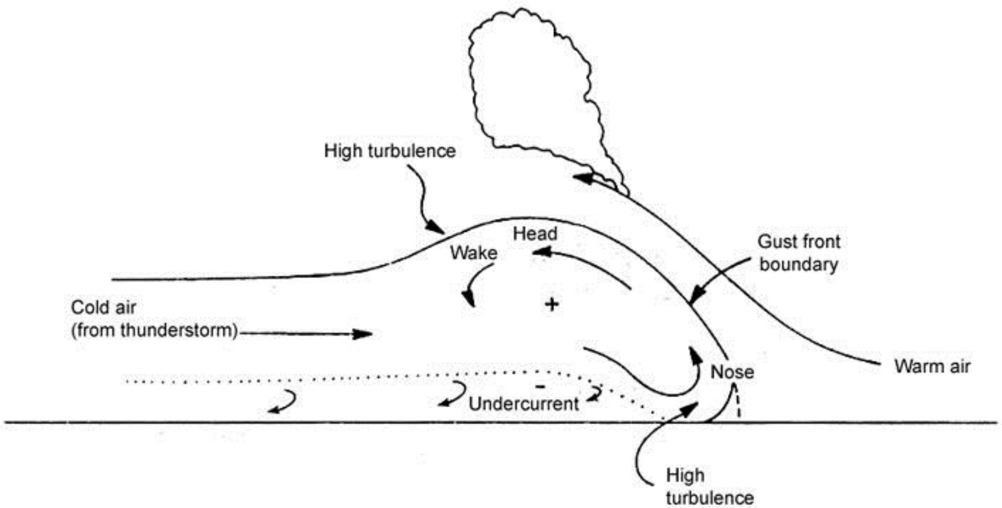

Schematic diagram of thunderstorm outflow, a type of gravity current (after Goff 1976)

Powder snow avalanche gravity current (Simpson 1987)

Evolution of a Gravity Current into a Bore

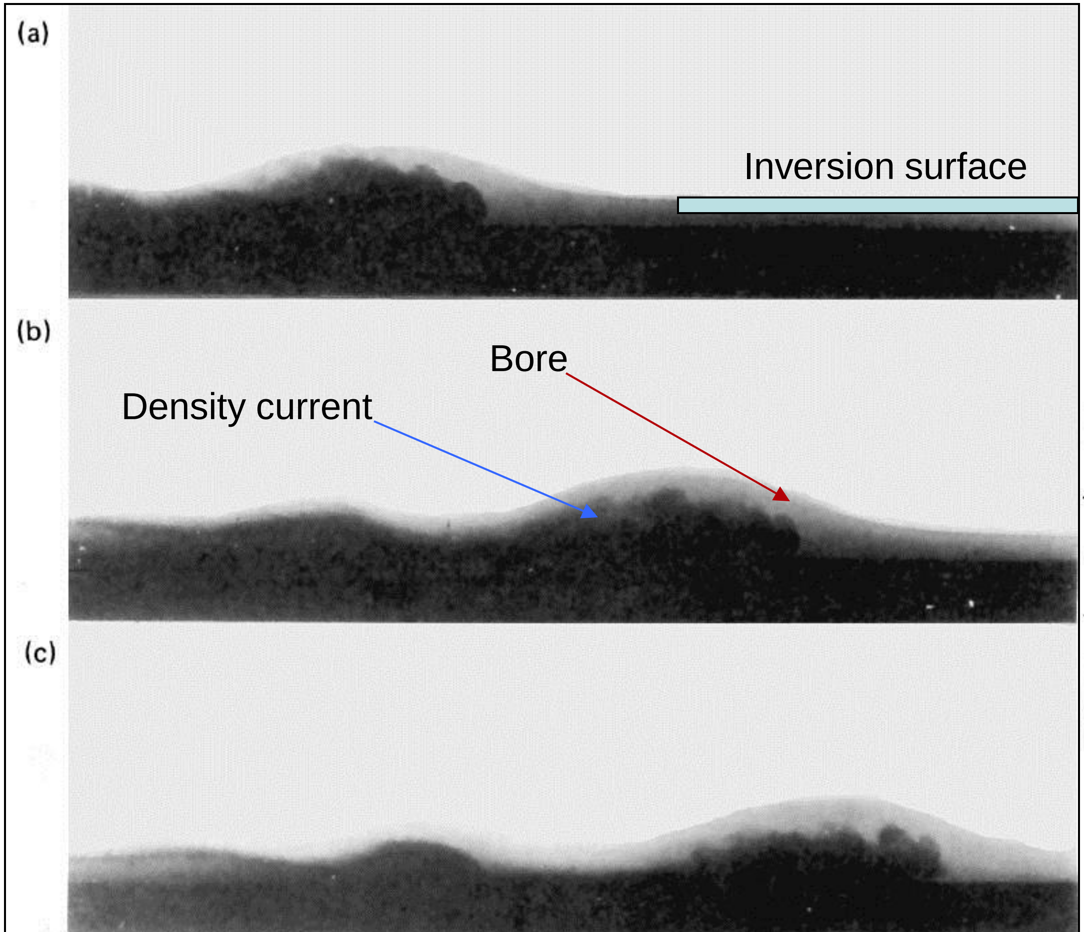

Evolution of an undular bore from an advancing gravity current (Simpson 1987). Fluid enveloping the current is similar to what happens to warm air underneath a low-level inversion as a gravity current intrudes into the inversion.

An internal bore in the atmosphere is a type of gravity wave generated by the intrusion of a gravity current into a ground-based stable layer.

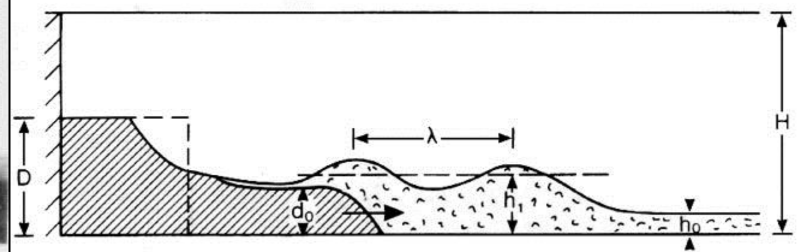

Generation of an internal bore of depth h_1 by an advancing gravity current of depth d_0 intruding into a stable layer of depth h_0

Passage of the bore results in a sustained elevation of the stable layer. Unlike gravity currents, bores do not transport mass.

Evolution of a Bore into a Soliton

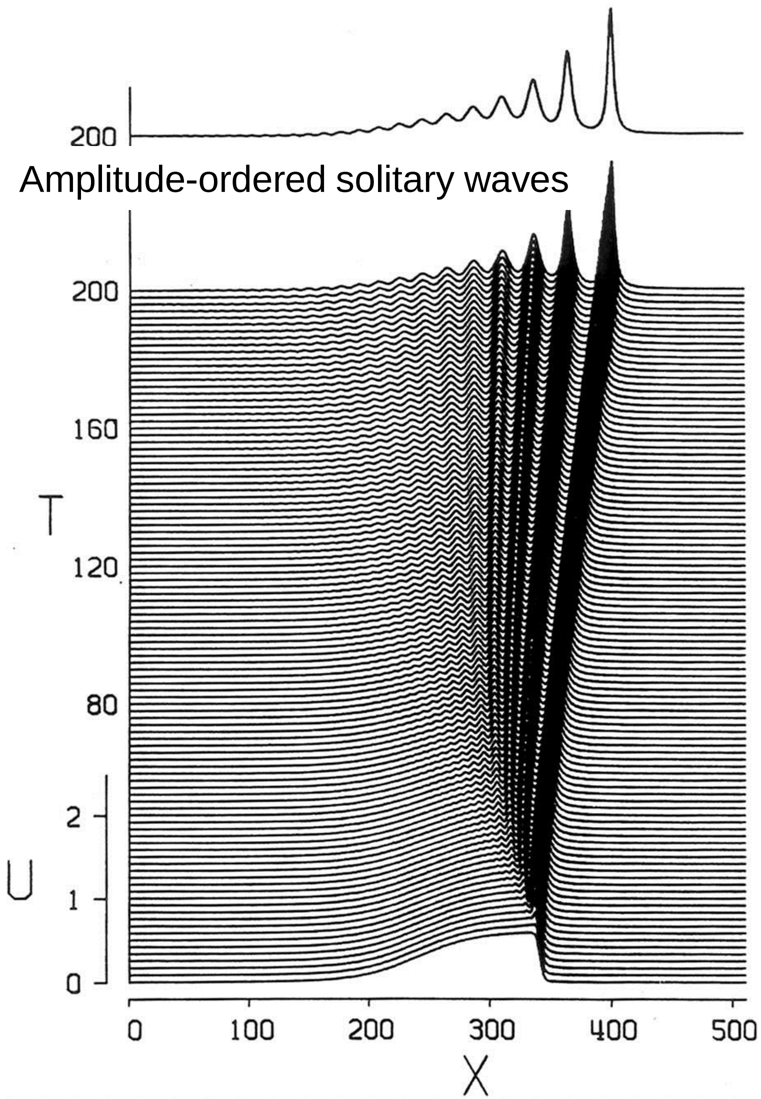

Solution of the BDO equation for deep-fluid solitary waves from an initial wave of elevation along an inversion in a waveguide embedded in a neutrally stable fluid of infinite extent (Christie 1989)

A train of amplitude-ordered solitary waves (or soliton) can evolve from stronger bores in some instances. Wave amplitudes vary inversely with their width.

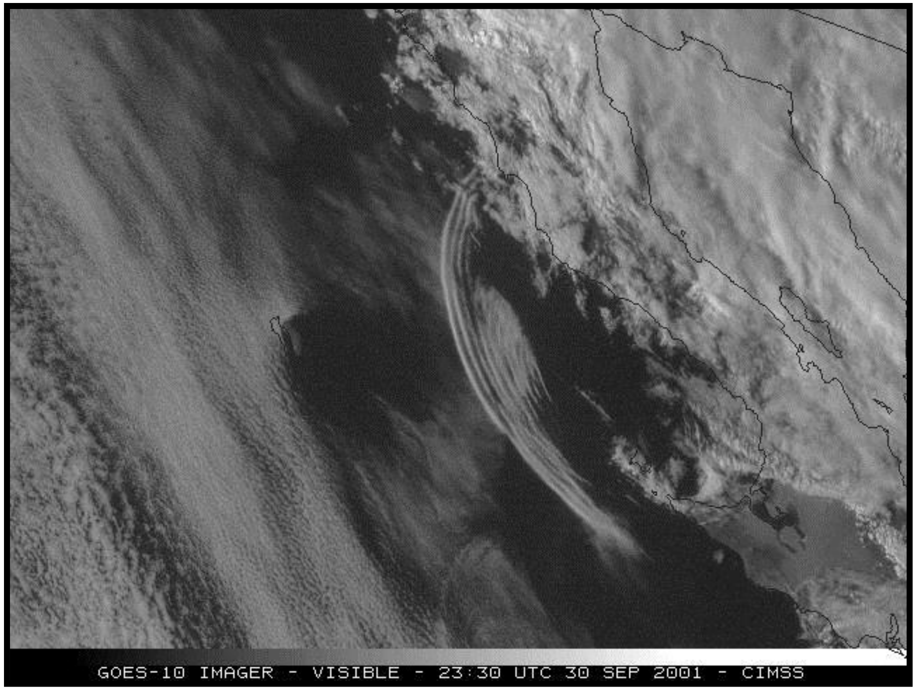

The number of waves increases with time, limited by turbulent dissipation. The energy of the wave system tends to be concentrated in the first few solitary waves.

Types of Bores

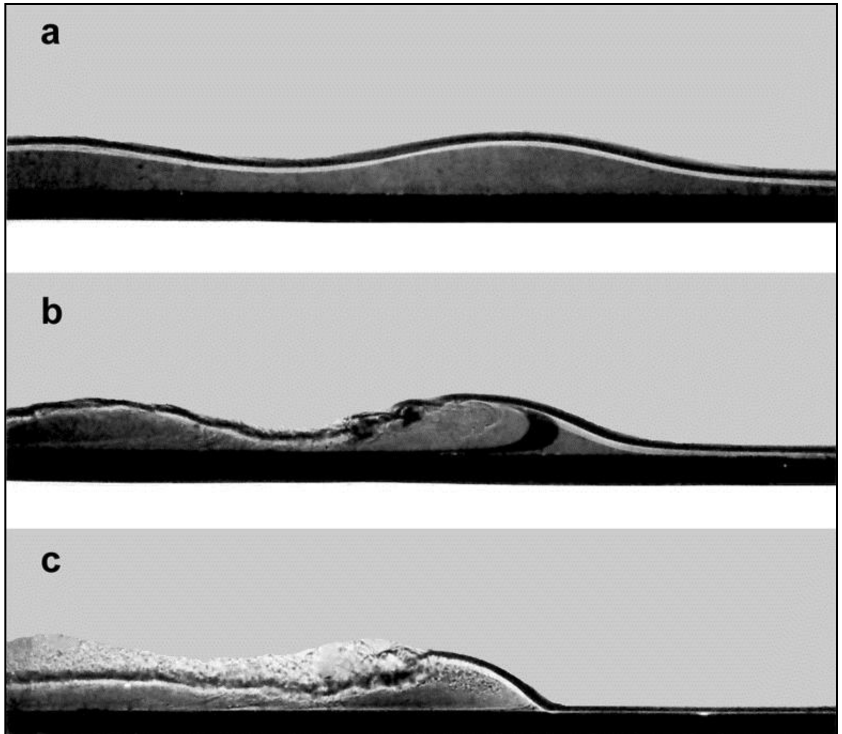

Transition of an undular bore to a turbulent bore at an interface between two fluids as bore strength increases from 1.5 to 3.0 to >4.0

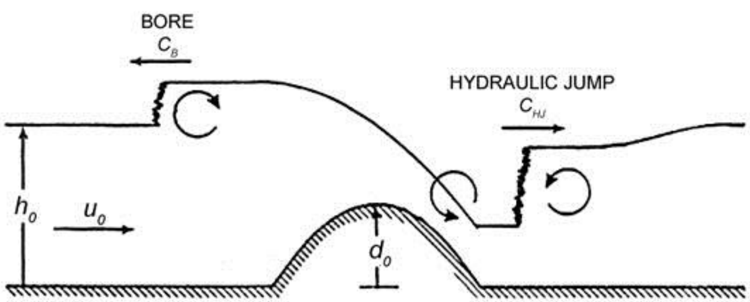

Schematic of shallow-water flow over a barrier depicting the upstream-propagating bore and downstream-propagating jump (Klemp et al. 1997)

Transition of an **undular** bore into a **turbulent** bore depends upon its strength (h_1 / h_0). Bore strength is determined by the Froude Number and the ratio of the gravity current depth to the inversion depth (d_0 / h_0). Stronger bores propagate faster with stronger, but shallower inversions.

Houghton and Kasahara (1968)

$$C_{bore} = C_{gw}\sqrt{0.5(d_b/h_0)(1+d_b/h_0)}$$

$$= Nh_0\left[0.5(d_b/h_0)(1+d_b/h_0)\right]^{1/2}$$

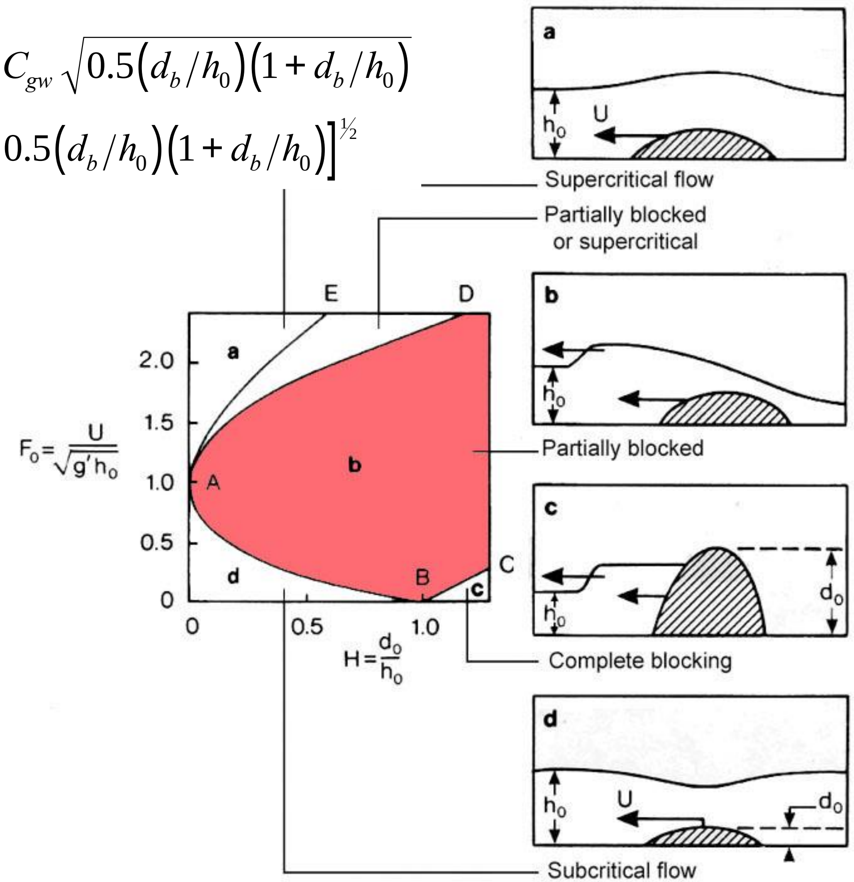

Four types of disturbances that can be generated by a moving obstacle at the interface between two fluids (hydraulic theory)

WAVE DUCTING: Needed to maintain bores

According to the wave dispersion equation, upward propagating (internal) plane waves in the absence of the Coriolis force can only occur if intrinsic frequency $v < N$.

$$m^2 = \frac{N_m^2}{(U - C_b)^2} - \frac{\partial^2 U / \partial^2 z}{(U - C_b)} - k^2$$

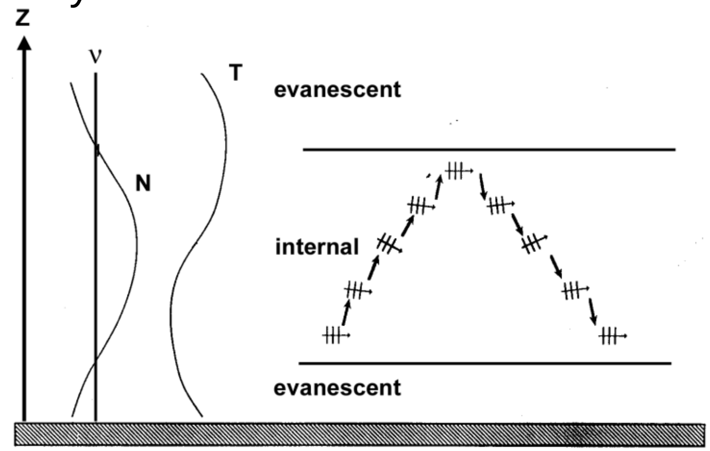

Stability (first) term of Scorer parameter:

$$m^2 = \left(\frac{N}{n}\right)^2 k^2 = \left[\frac{N}{k(C - U)}\right]^2 k^2 = \left(\frac{N}{C - U}\right)^2$$

At the "critical level", where $C = U$, the waves are "trapped" from upward propagation, provided that the stable layer is deeper than 25% of the vertical wavelength and Ri < 0.25.

Two parameters determine whether a bore will be generated from an intrusive gravity current:

- ⌠ > 0.7 (ratio of long gravity wave speed to density current speed)
- Large Froude Number (ratio of relative speed to densimetric speed)

$$F = \frac{(U - C_{gc})}{C_*} = \frac{(U - C_{gc})}{\sqrt{g \mathrm{D} q d_0 / q_{vw}}}$$

$$d_{dc} = \frac{\theta_{vc} \Delta p}{\rho_w g[(p_c/p_w)\theta_{vw} - \theta_{vc}]} \cong \left(\frac{C_{dc}}{\mathrm{Fr}}\right)^2 \left(\frac{\theta_v}{g \Delta \theta_v}\right)$$

$$m = \frac{C_{gw}}{C_{gc}} = \frac{2Nh_0/p}{C_{gc}}$$

$$C_{dc} = \mathrm{Fr}\left(\frac{\Delta p}{\rho_w}\right)^{1/2} \approx \mathrm{Fr}\left(g d_{dc} \frac{\Delta \theta_v}{\theta_v}\right)^{1/2}, \quad \text{and}$$

The Pre-Frontal Bore Event of April 26,1991:

A case of CI caused by a bore

(Koch and Clark, 1999 J. Atmos. Sci.)

Low-level radar displays & mesonet data

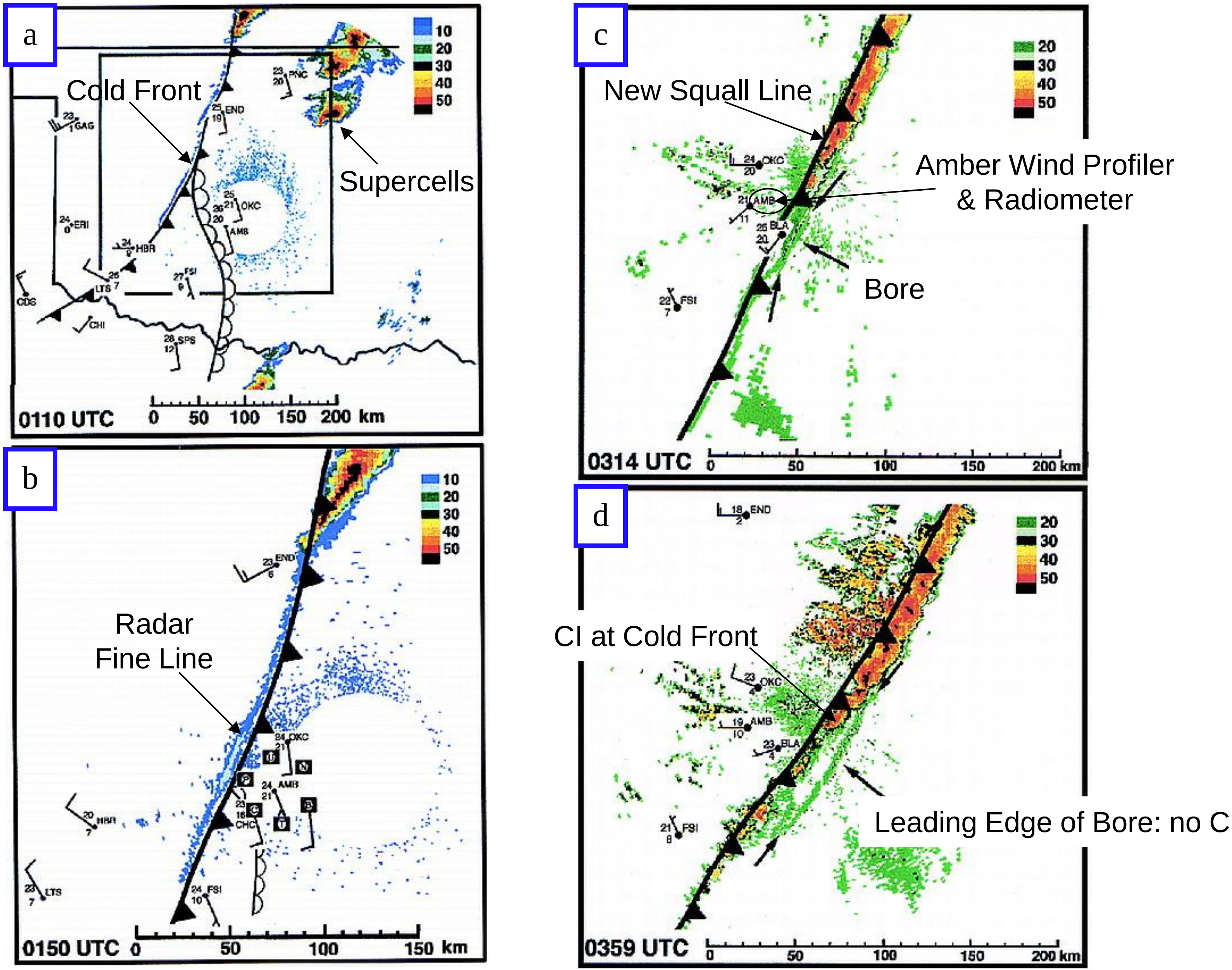

Surface mesonet traces from Amber, OK and microwave radiometer traces

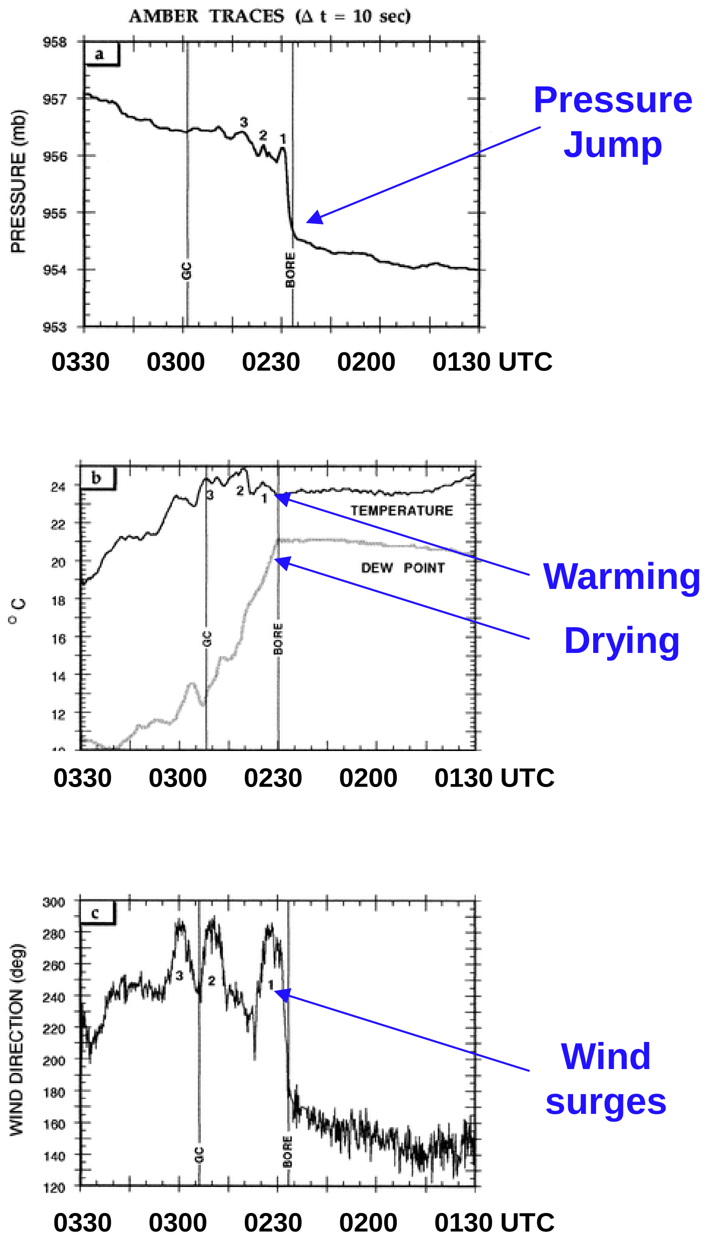

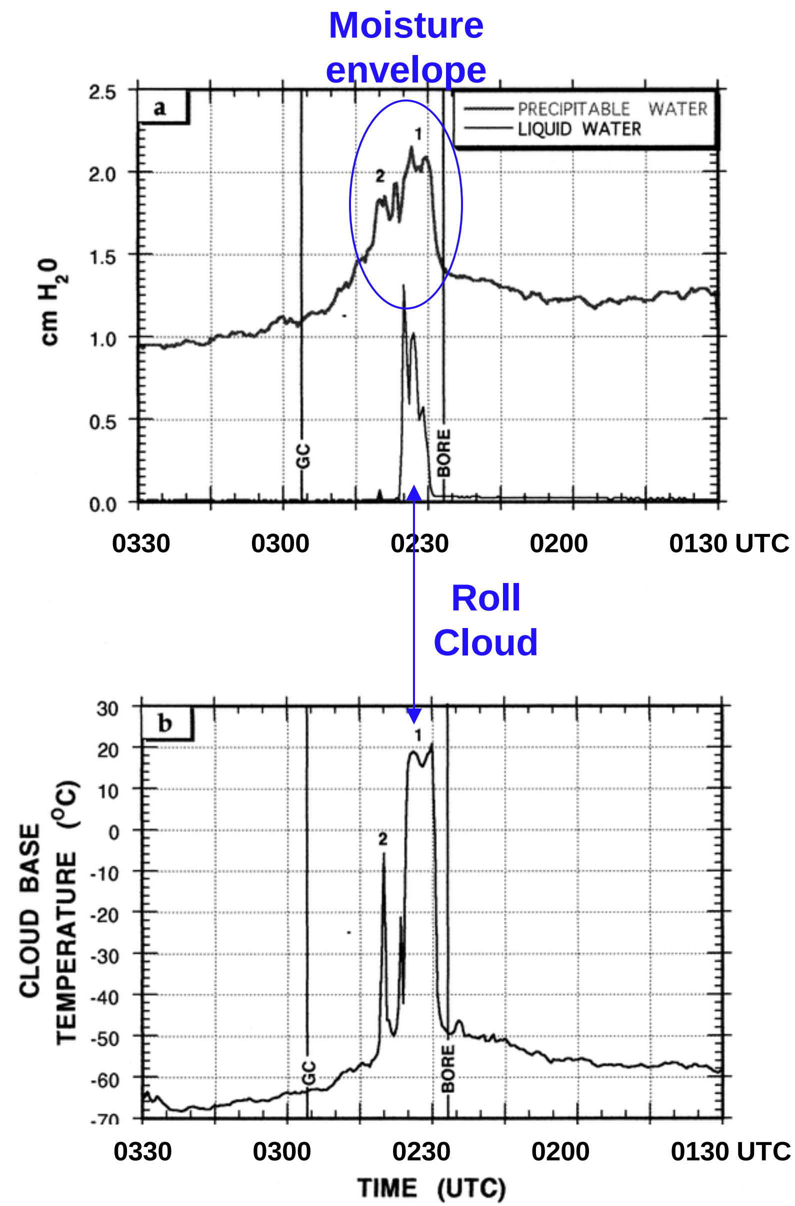

Derived two-dimensional circulation system from 915-MHz wind profiler relative to the bore and gravity current-like cold front

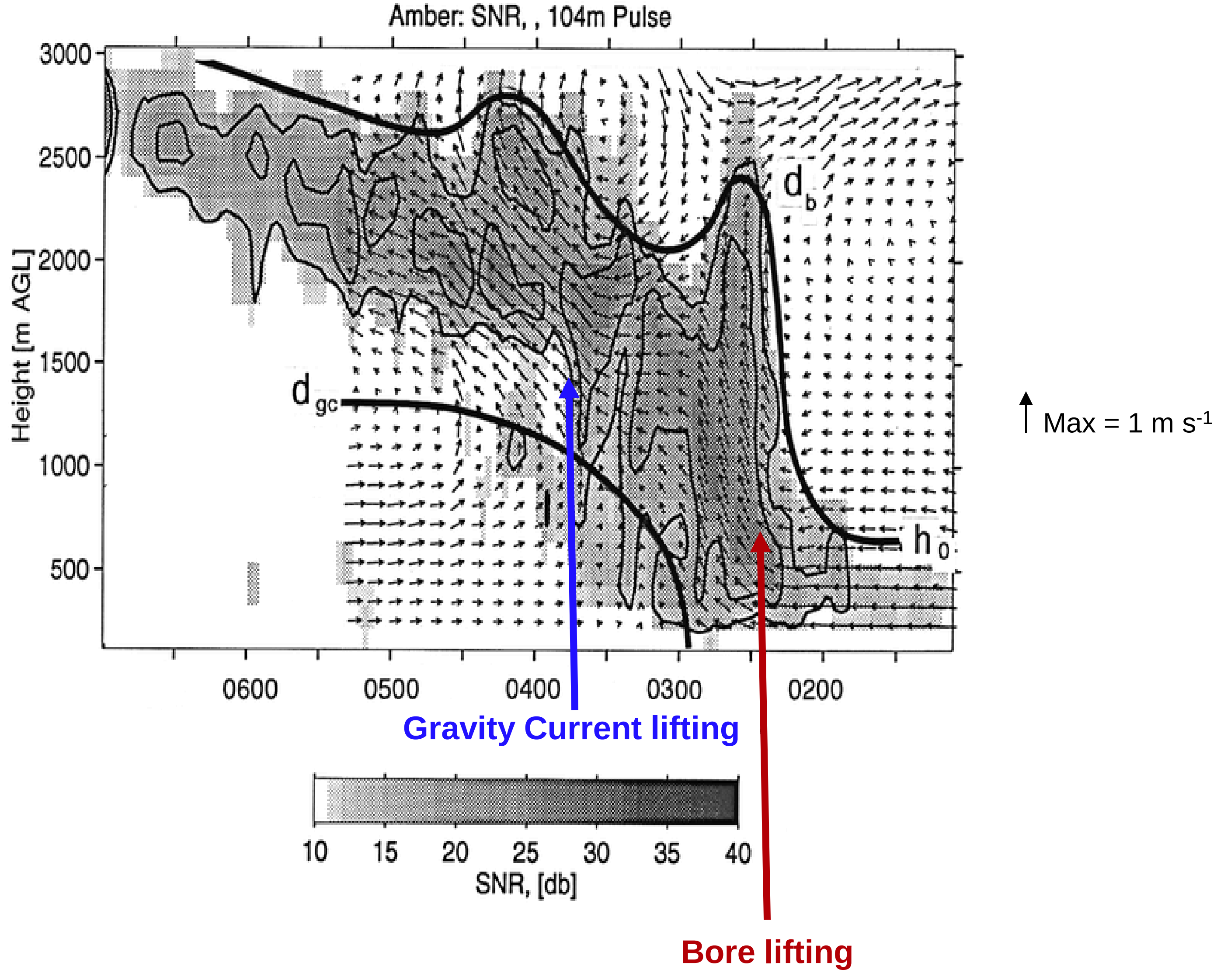

Combined lifting by bore and gravity current-like cold front destabilizes and moistens sounding above the surface: convection initiated

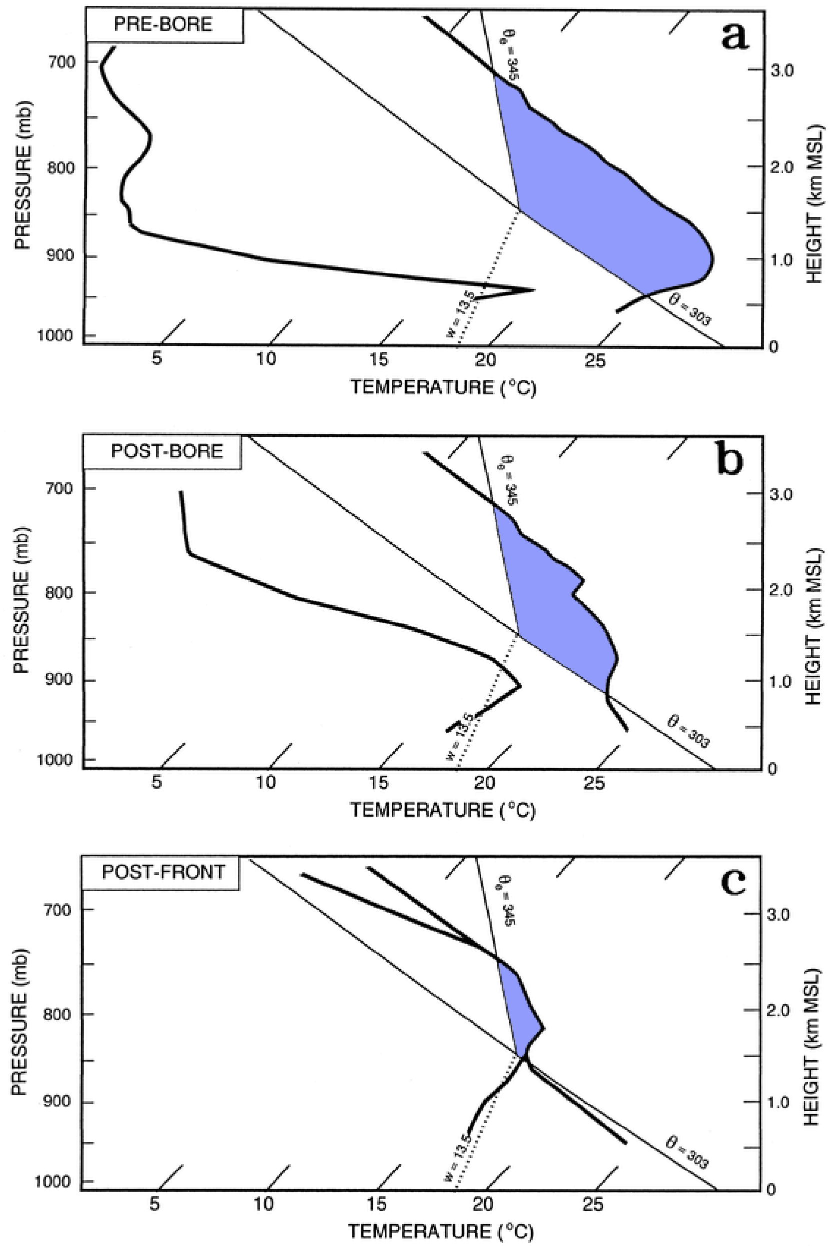

Max displacement = 1.25 km

Lifting depth = 2.5 km

(bore + front combined)

The Bore-Soliton Event of June 20, 2002

No CI in this case

(Koch et al., 2008 J. Atmos. Ocean. Tech.)

IHOP_2002 (International H_20 Project) Surface Measurement Platforms used to study bores

Homestead observing systems used:

- ✓ **ISS**: NCAR Integrated Sounding Systems (3-h soundings) and surface 1-5 min mesonetwork data
- ✓ **S-POL**: S-band Doppler radar with refractivity estimates
- ✓ **GLOW**: Goddard Lidar Observatory for Winds (Doppler Lidar) @ 1.3-km horiz. and 150 m vert. resolution
- ○ **AERI**: Atmospheric Emitted Radiance Interferometer @10 min, 50-250 m resolution
- ✓ **FM-CW** 10-cm radar with 2-m resolution
- ○ **MAPR**: 915 MHz Multiple Antenna Profiler @30-sec, 60-m resolution
- ✓ **HARLIE**: aerosol backscatter lidar
- ✓ **SRL**: Scanning Raman Lidar @ 2 min, 60m resolution

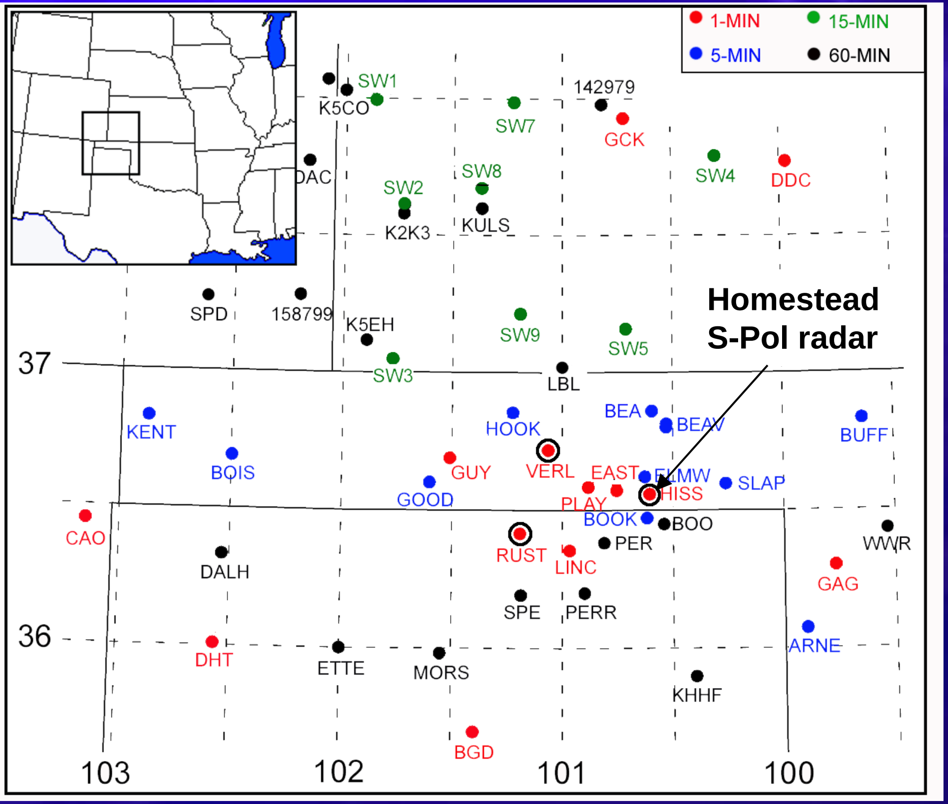

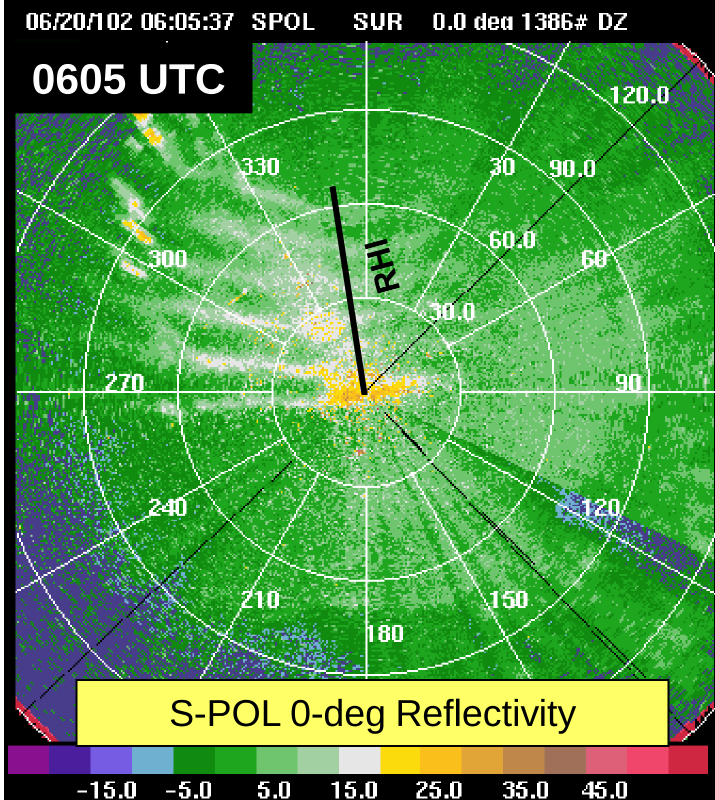

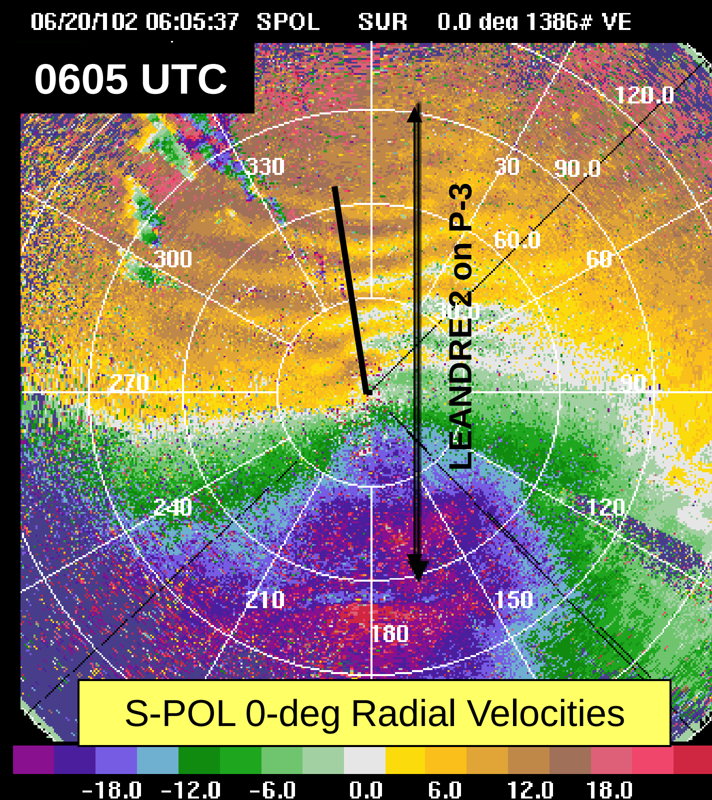

Leandre2 DIAL water vapor mixing ratio retrievals:
800 m horizontal resolution
300 m vertical resolution

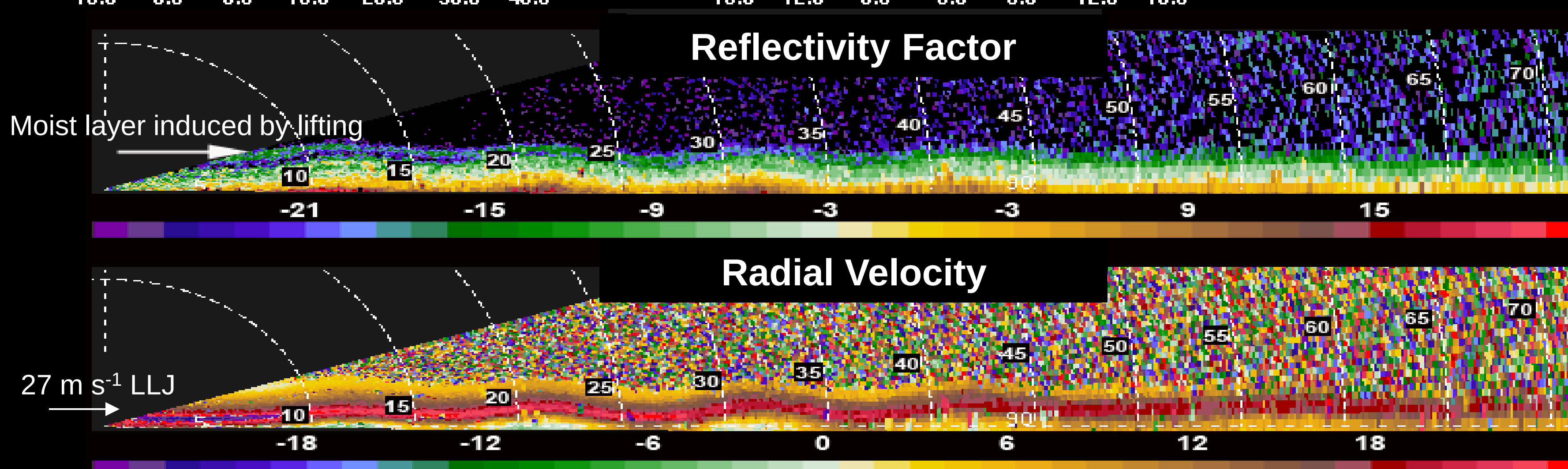

S-POL RHIs at 0530 UTC along azimuth 350°

LEANDRE 2 : 3rd pass (0408-0427 UTC)

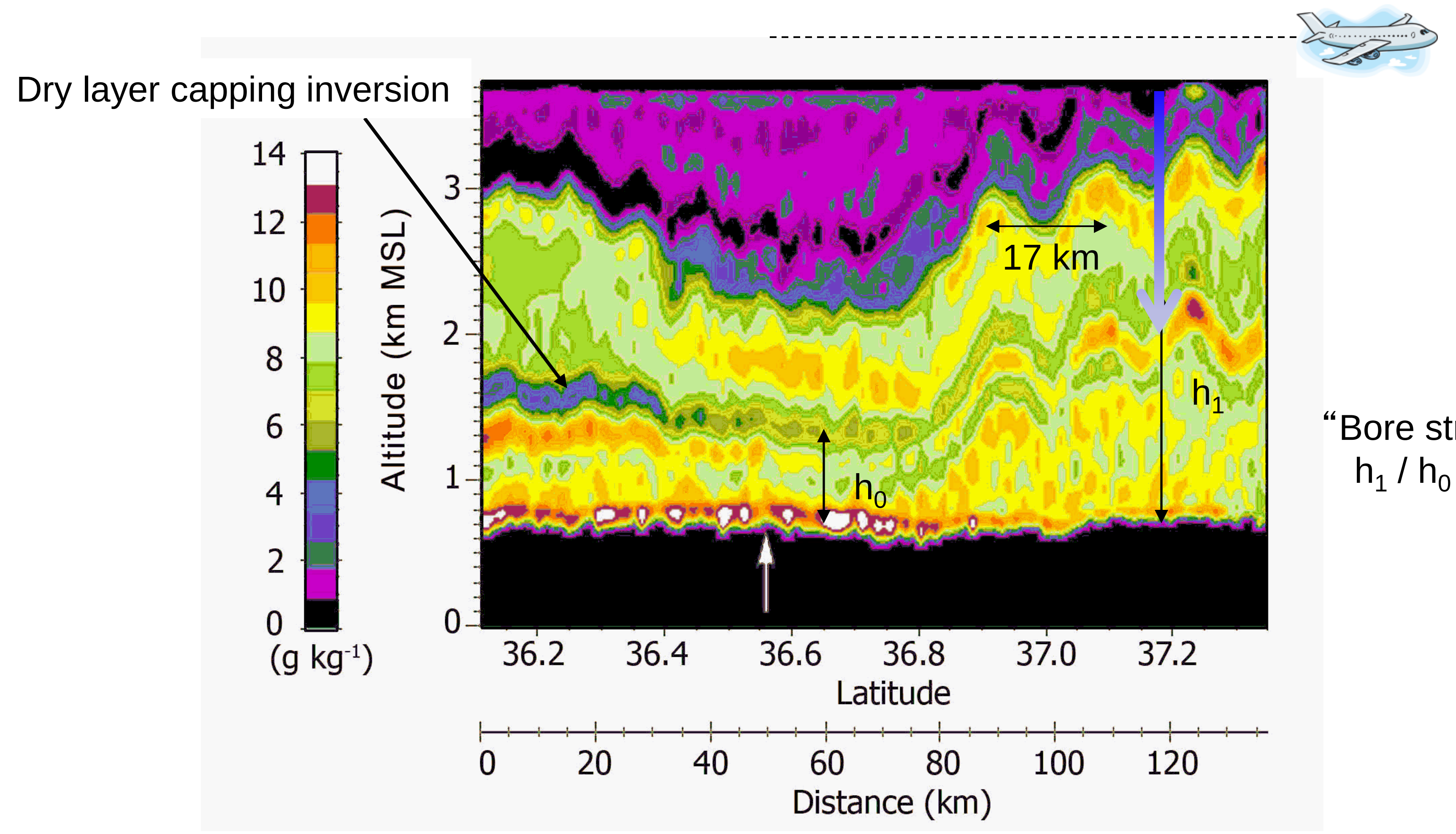

"Bore strength"
$h_1 / h_0 \sim 2.1$

- Amplitude ordered solitary waves (leading wave is strongest)
- Inversion surface (h_0) lifted successfully higher by each passing wave
- Wave ducting (trapping) mechanism suggested by lack of tilt of waves with height

Circulation transverse to the bore derived from Doppler Wind Lidar

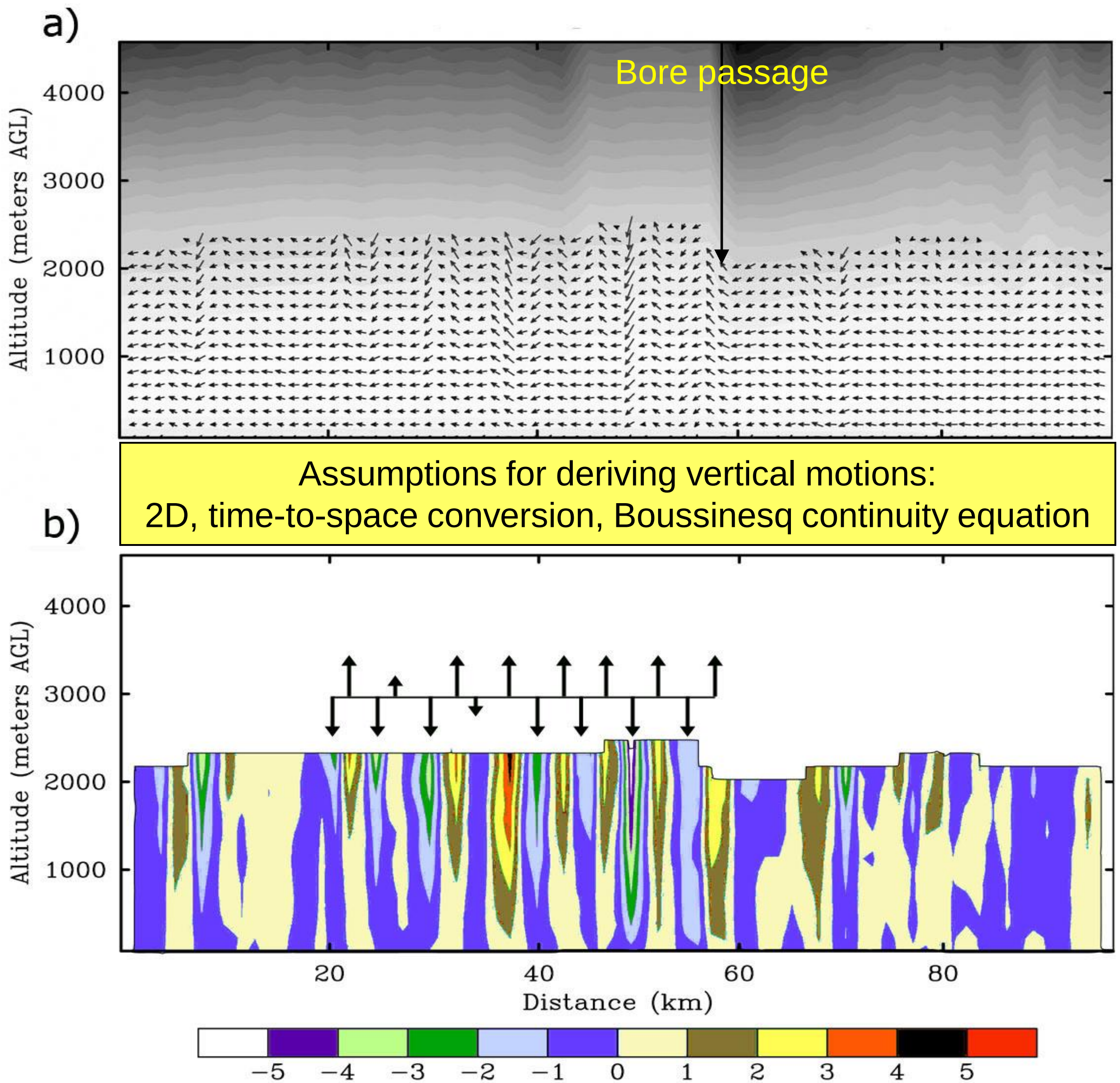

Shading = average photon count values

Vectors = bore-relative 2D winds

2 m s^{-1} max upward motion agrees with MAPR spaced antenna profiler

Application of GLOW vertical velocity over wave period of 16 min produced 400–700 m lifting below 2.5 km altitude - in agreement with Leandre2

Bore ducting analysis for 0602 UTC 20 June 2002

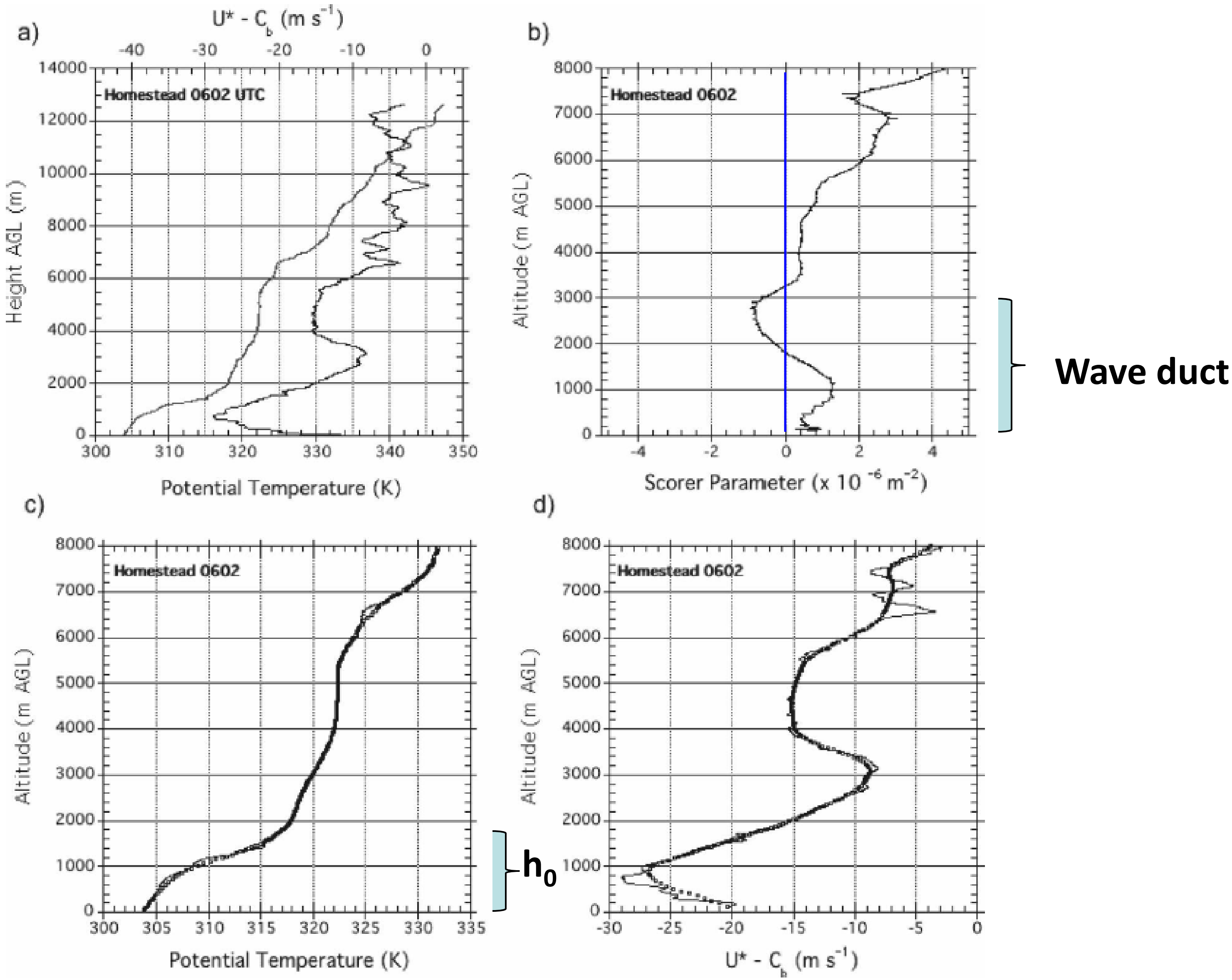

Despite wave duct and computed 2 m/s vertical velocity from GLOW/MAPR, this was insufficient to trigger convection (result was < 700 m lifting by leading wave, about half that estimated in 26 April 1991 case)

The Dual Bore Event of June 4, 2002

A case of local CI by a bore

(Koch et al., 2008 Mon. Wea. Rev.)

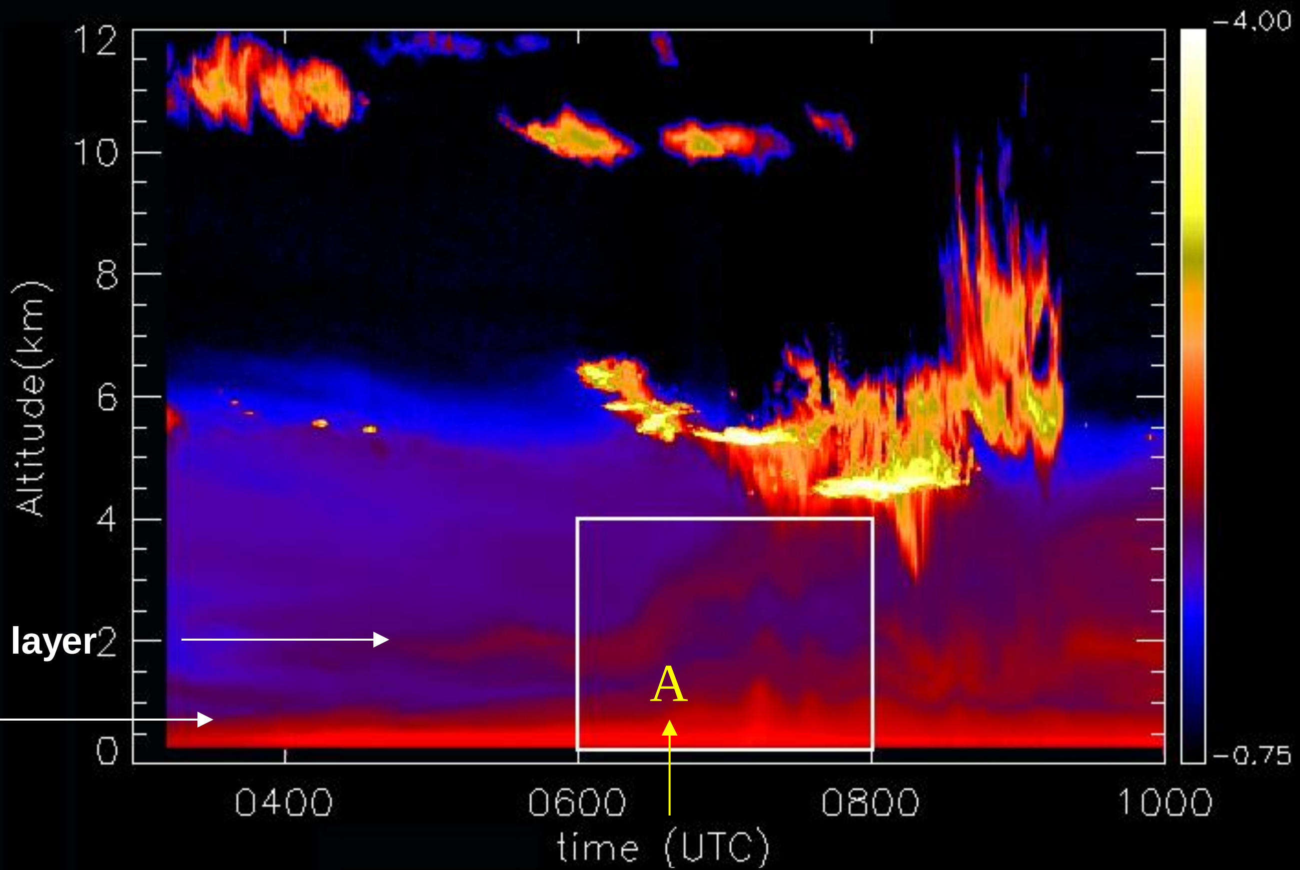

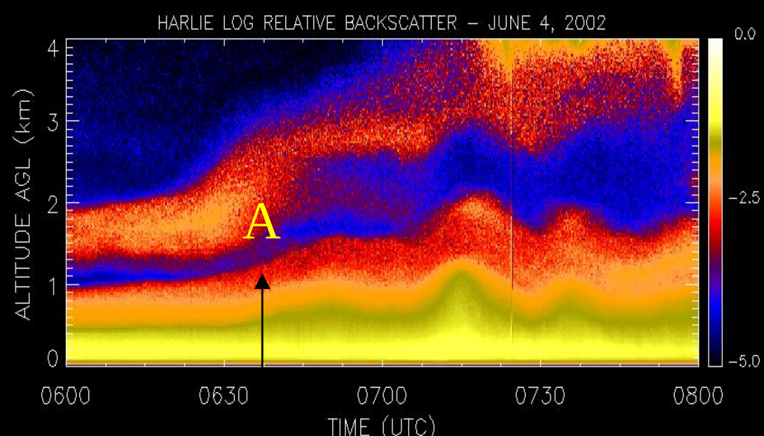

HARLIE aerosol backscatter lidar: deep lofting of aerosols by bore A

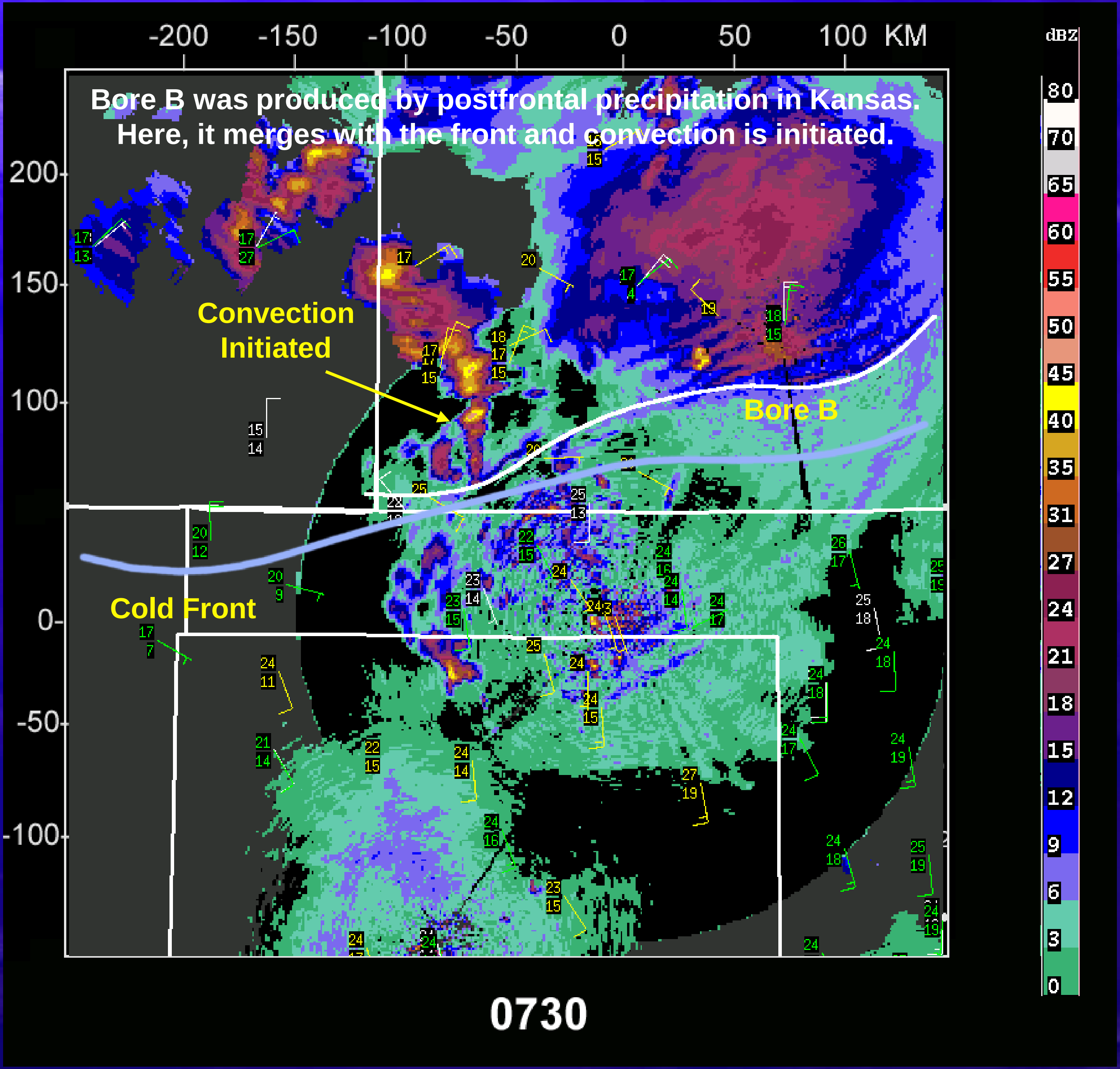
Bore B was produced by postfrontal precipitation in Kansas.
Here, it merges with the front and convection is initiated.
Convection Initiated
Bore B
Cold Front
-200
-150
-100
-50
0
50
100 KM
200
150
100
0
-50
-100
dBZ
80
70
65
60
55
50
45
40
35
31
27
24
21
18
15
12
9
6
3
0
0730

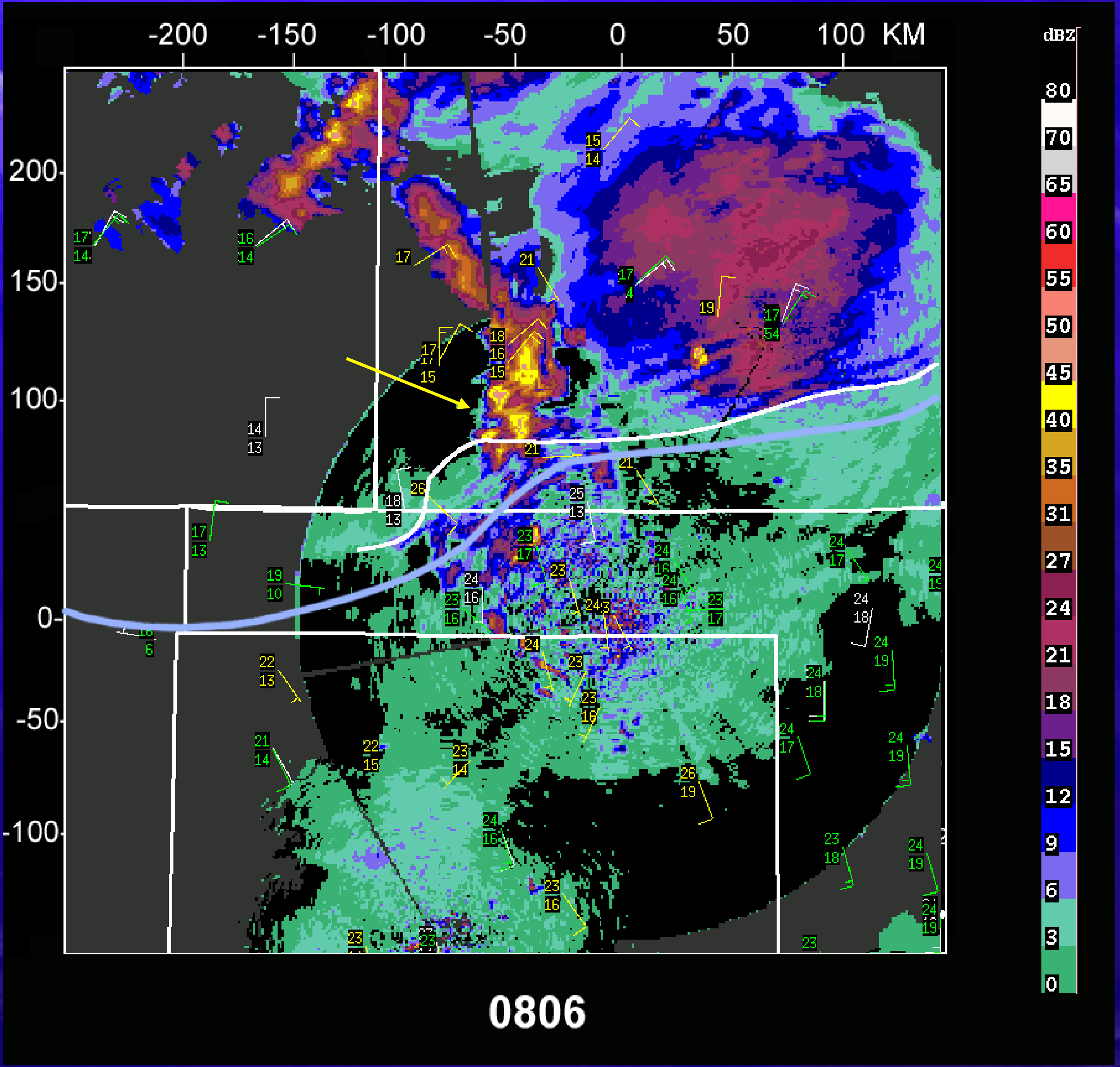

-200 -150 -100 -50 0 50 100 KM
200
150
100
0
-50
-100
dBZ
80
70
65
60
55
50
45
40
35
31
27
24
21
18
15
12
9
6
3
0
0806

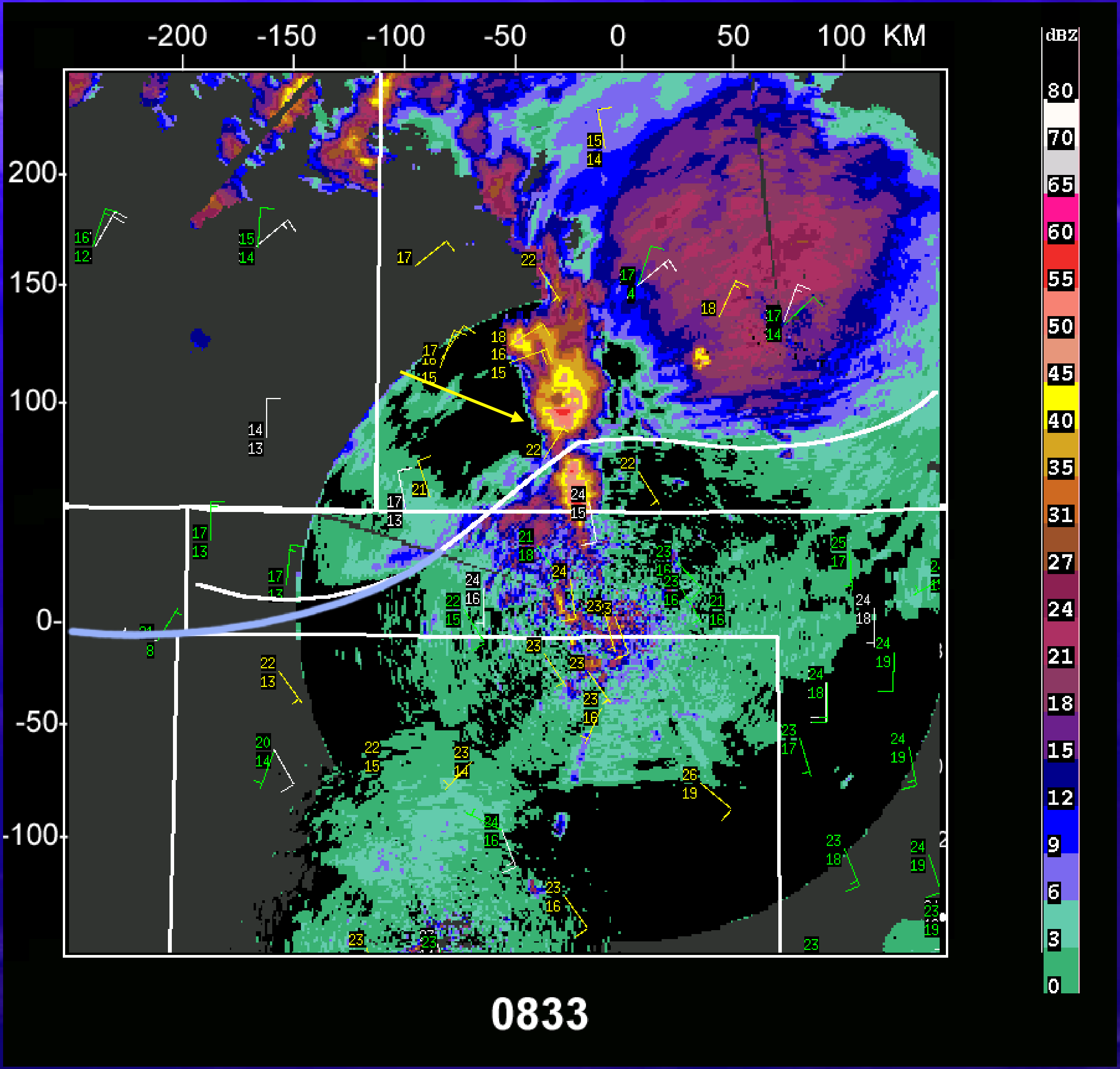

-200
-150
-100
-50
0
50
100 KM
200
150
100
0
-50
-100
dBZ
80
70
65
60
55
50
45
40
35
31
27
24
21
18
15
12
9
6
3
0
0833

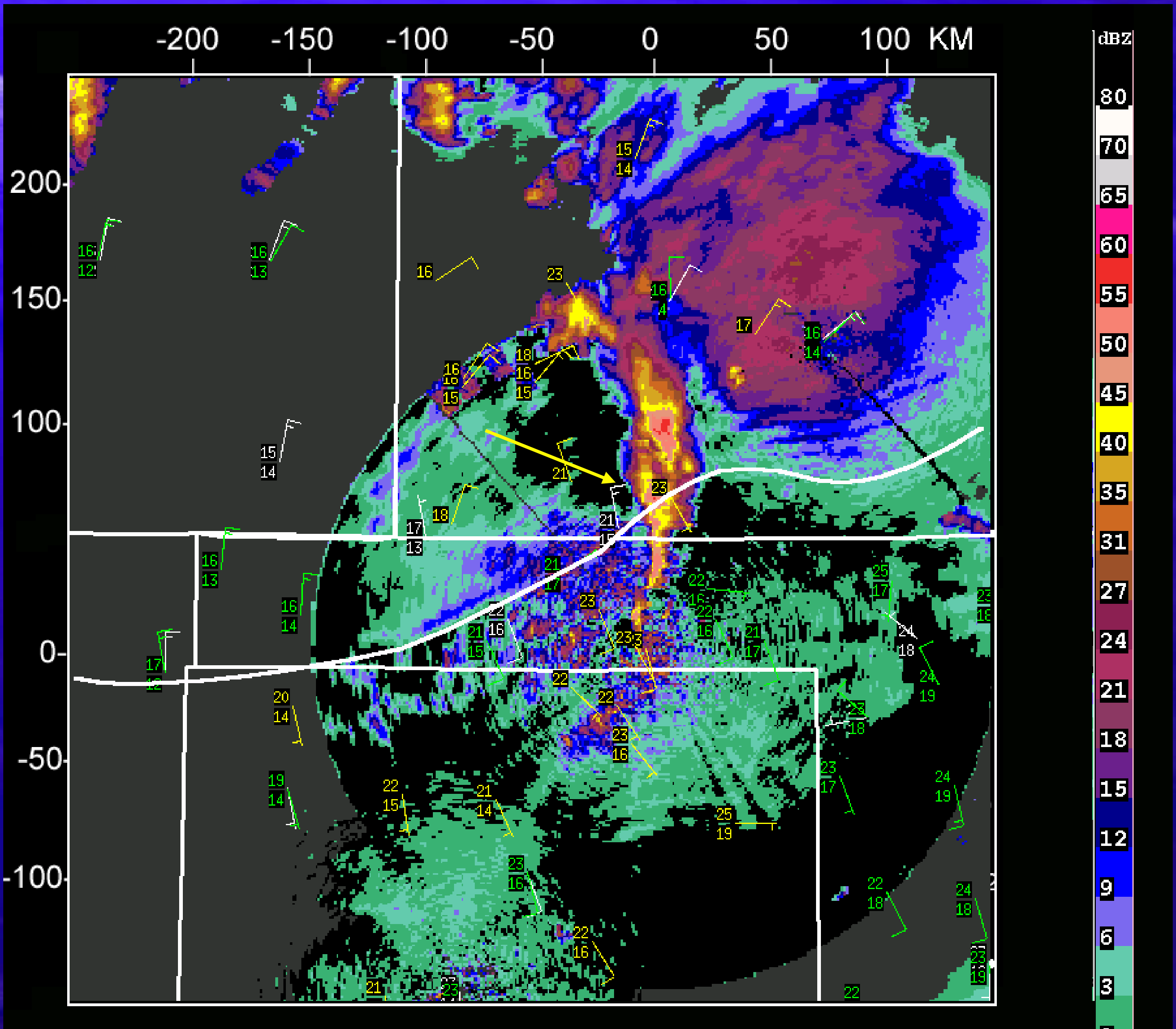
-200
-150
-100
-50
0
50
100
KM
200
150
100
0
-50
-100
dBZ
80
70
65
60
55
50
45
40
35
31
27
24
21
18
15
12
9
6
3
0

0900

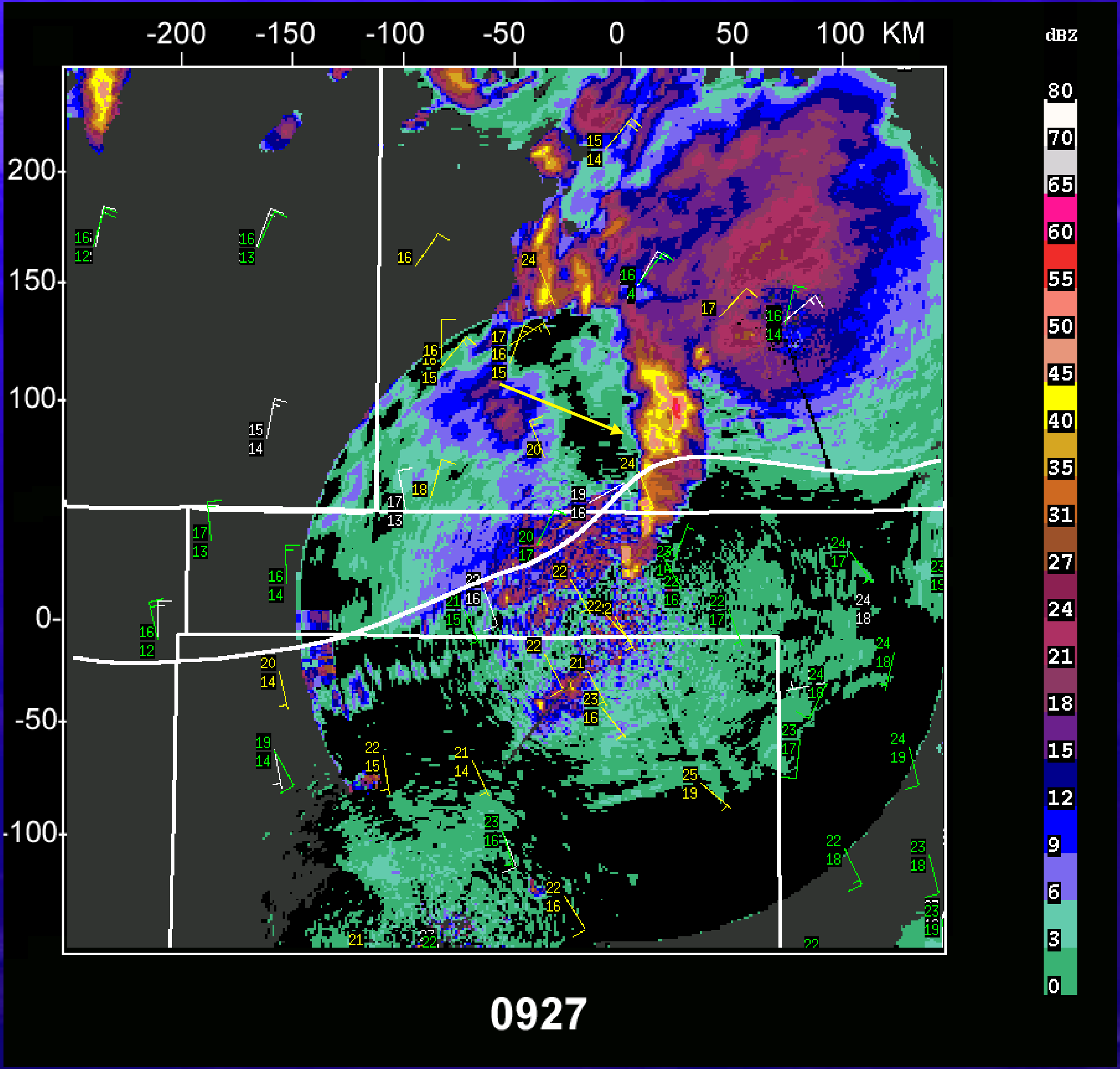
-200
-150
-100
-50
0
50
100
KM
200
150
100
0
-50
-100
dBZ
80
70
65
60
55
50
45
40
35
31
27
24
21
18
15
12
9
6
3
0
0927

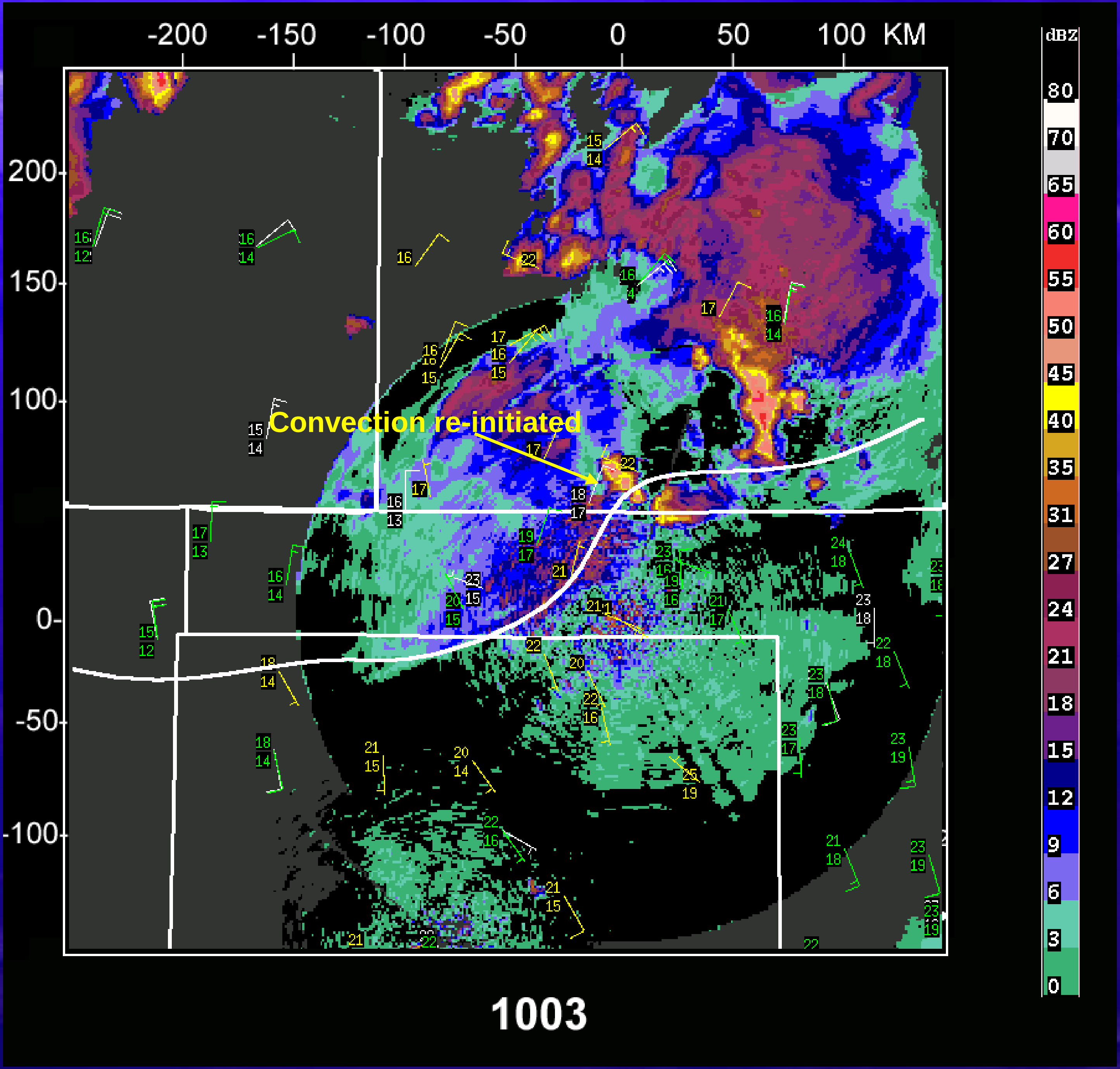
-200
-150
-100
-50
0
50
100
KM
200
150
100
0
-50
-100
dBZ
80
70
65
60
55
50
45
40
35
31
27
24
21
18
15
12
9
6
3
0
Convection re-initiated
1003

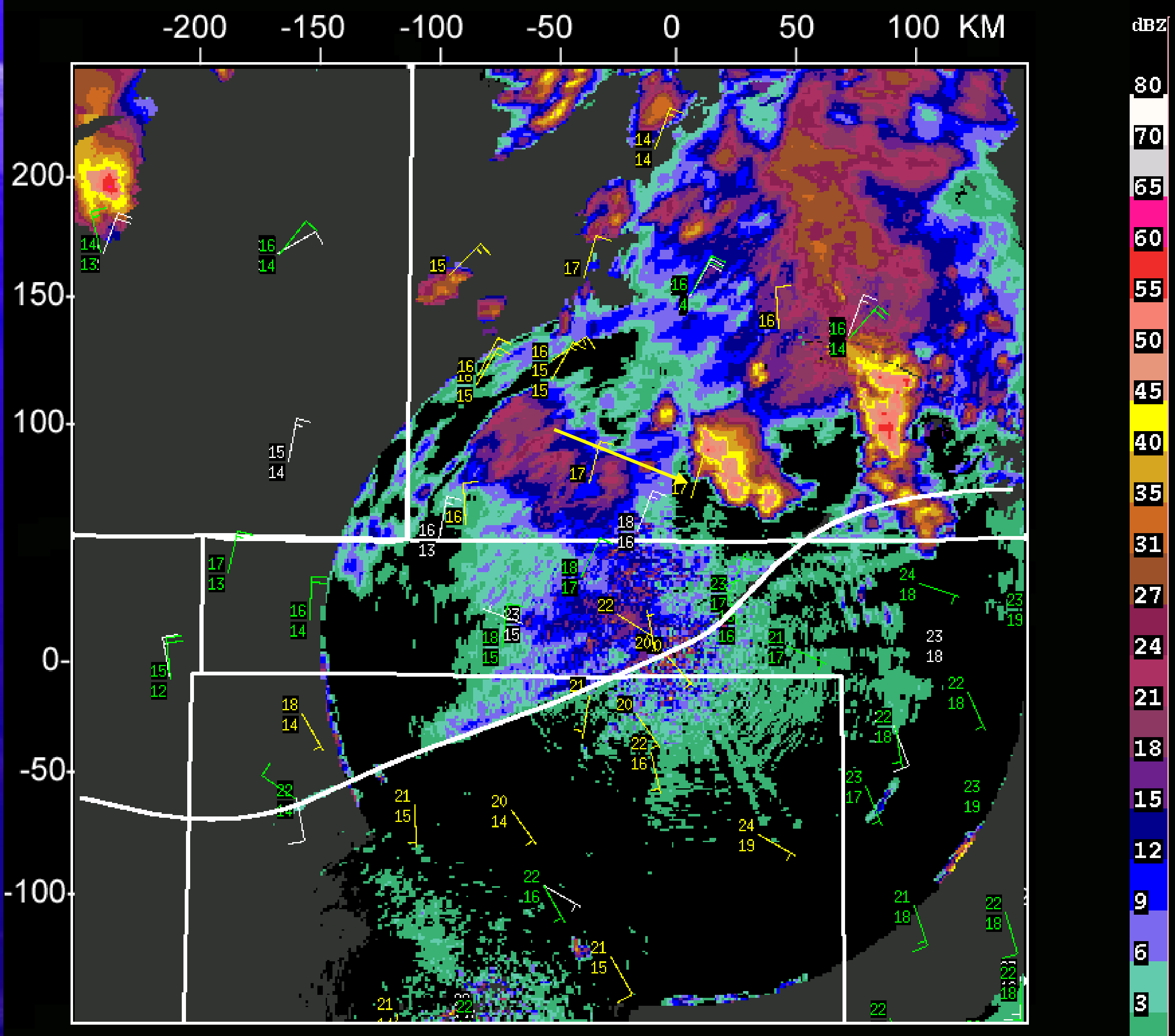
-200
-150
-100
-50
0
50
100
KM
200
150
100
0
-50
-100
dBZ
80
70
65
60
55
50
45
40
35
31
27
24
21
18
15
12
9
6
3
0

1030

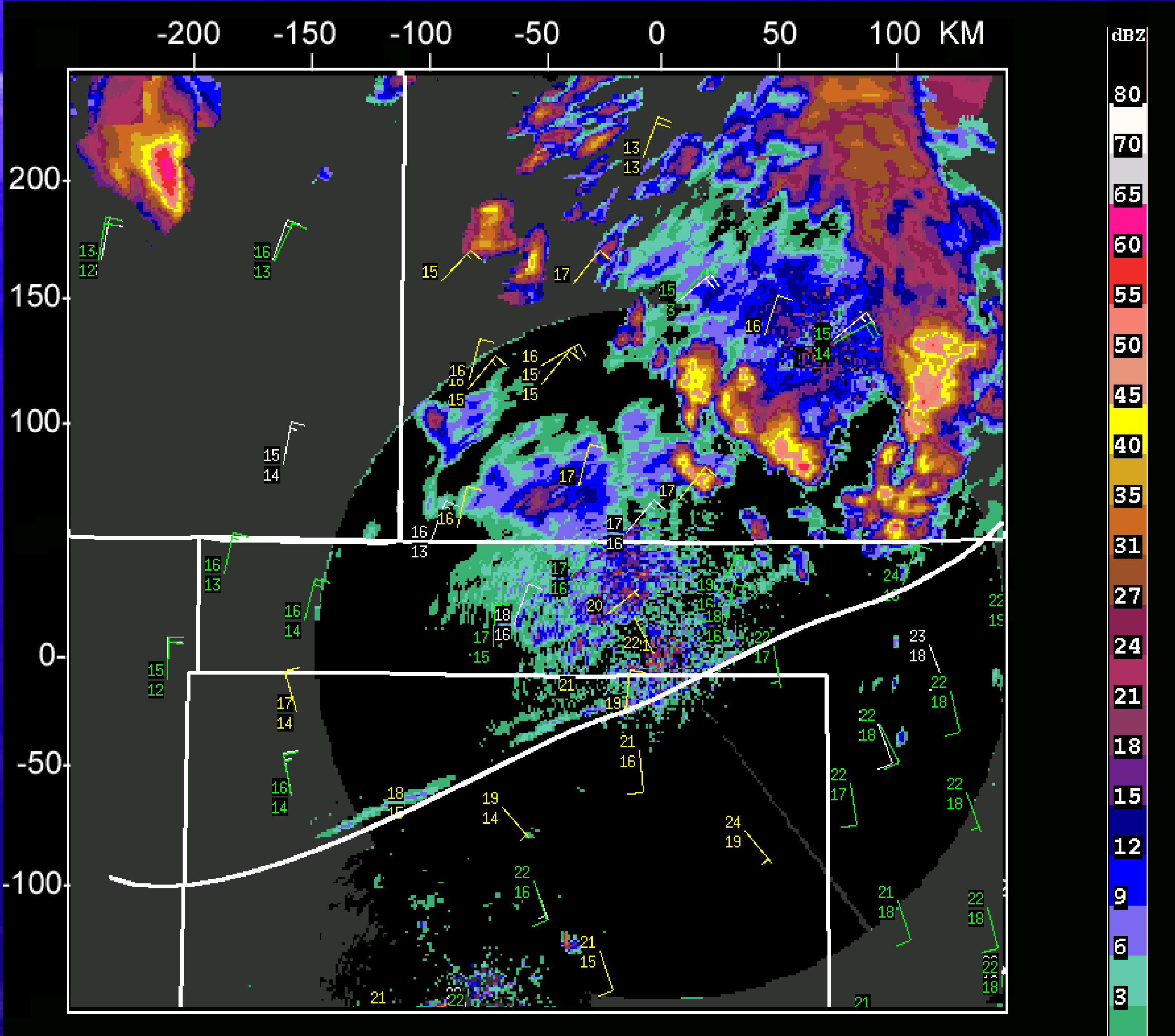
-200
-150
-100
-50
0
50
100
KM
200
150
100
0
-50
-100
dBZ
80
70
65
60
55
50
45
40
35
31
27
24
21
18
15
12
9
6
3
0

1106

Soliton B seen by FM-CW and Raman Lidar

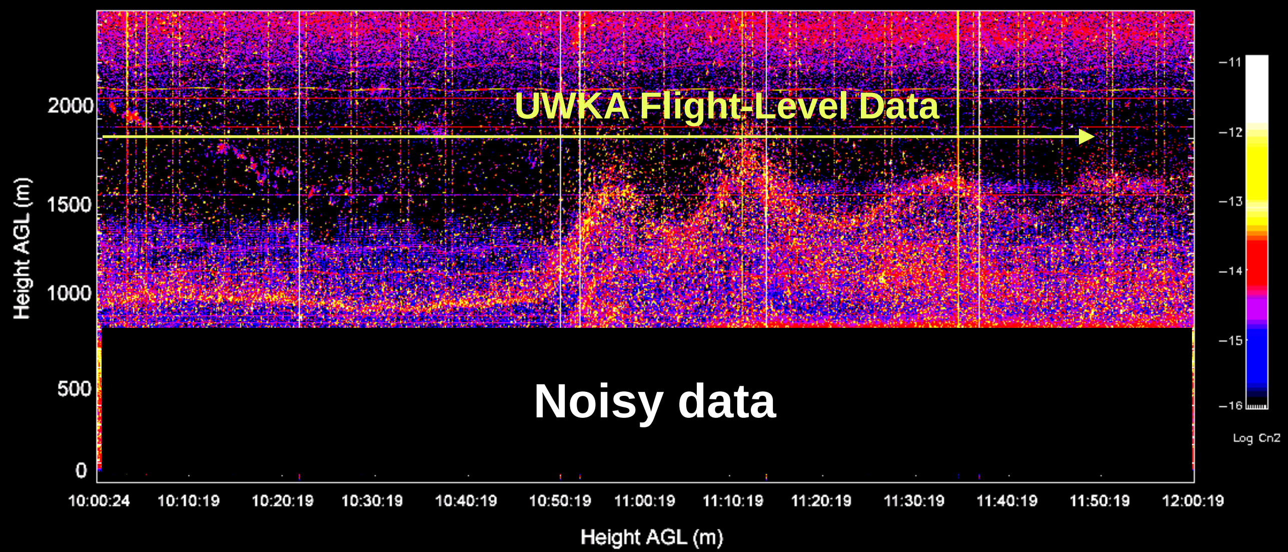

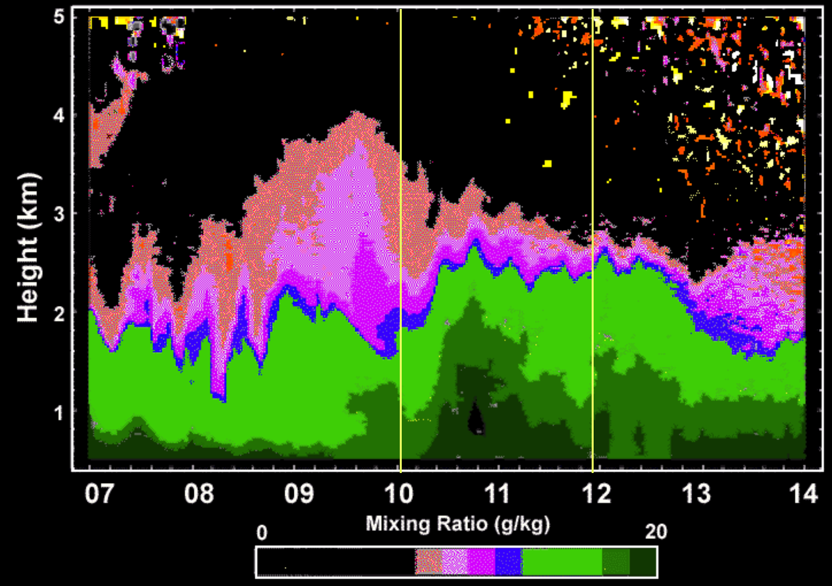

AERI thermodynamic soundings just before and after the dual bore event shows moistening and destabilization

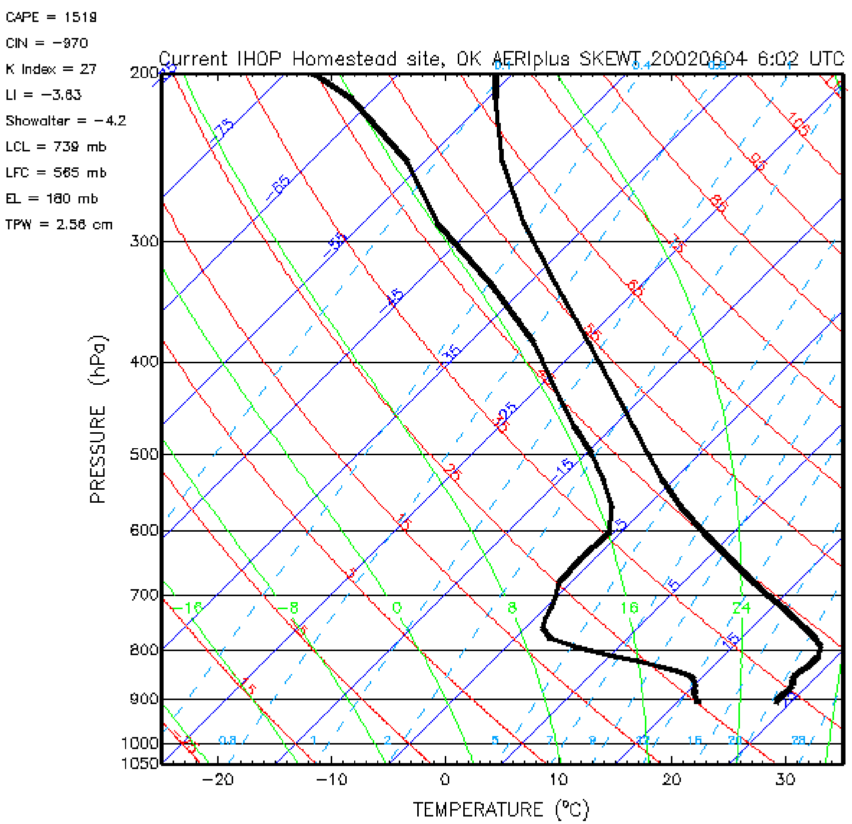

0602 UTC

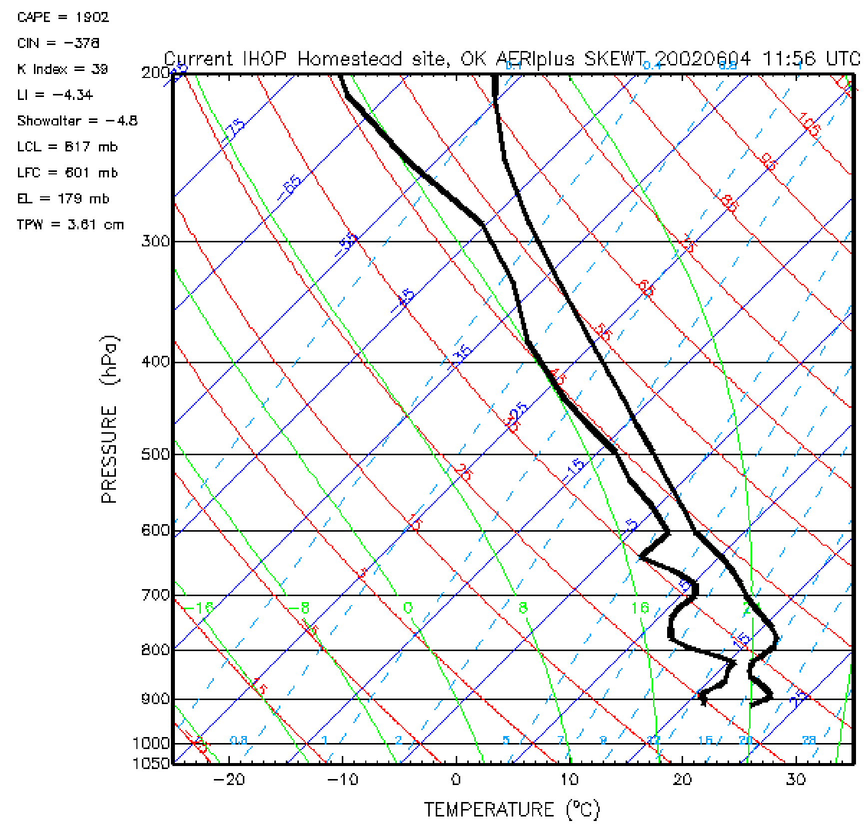

1156 UTC

Temporal variations in CAPE, CIN, and LCL from AERI hourly soundings prior to and after passage of both bores

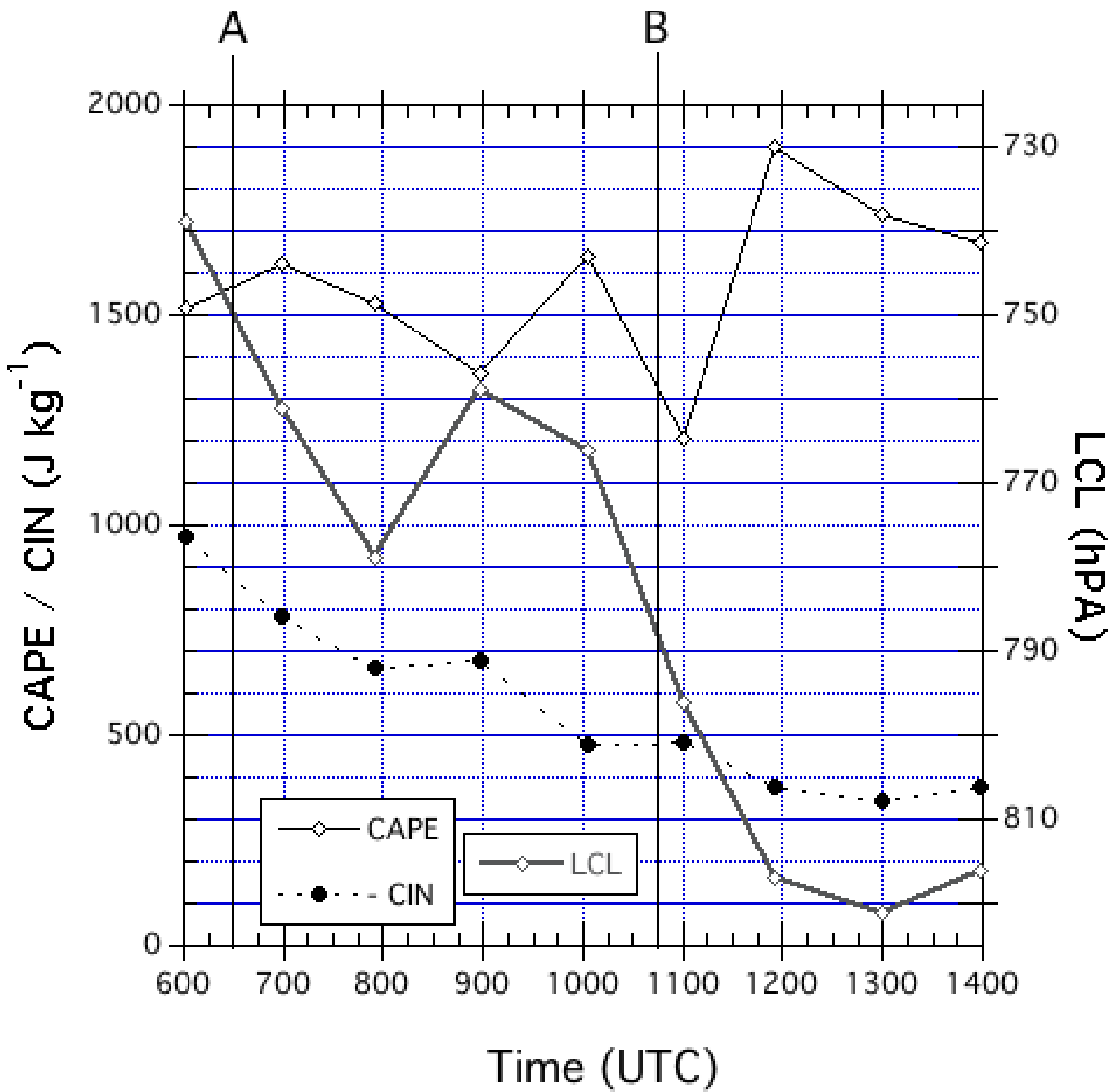

Conclusions about Bore CI Events

- In each case, the bores developed after formation of a strong nocturnal inversion in the presence of a very strong low-level jet. These phenomena together acted as the waveguide, helping to maintain longevity of the bore and subsequent soliton. This can serve as a tentative hypothesis for studies using PECAN datasets.

- Bores and solitons appeared as fine lines in radar reflectivity displays and their vertical structures were readily detected by airborne DIAL, and ground-based lidars and Doppler wind profilers. Other solitons have since been seen at NWC with our array of sensors, radars, and mesonet stations. Suggests PECAN success!

- Solitary waves developed to the rear of the leading fine line atop a 0.6-0.8 km deep surface stable layer. Depth of the stable layer approximately doubled with passage of the leading wave. The inversion was then further lifted by each passing wave. This process should be studied in greater depth using PECAN data & numerical models.

Conclusions

- A simple method for obtaining two-dimensional vertical circulations from Doppler lidar and UHF wind profiler data showed consistency with other lidar and radiometric measurements of water vapor fluctuation fields. PECAN to test?

- Application of derived vertical motions to local soundings correctly indicated ability of bore-induced lifting to trigger convection. These results indicate that though bores generated by gravity currents can produce strong lifting, this may be insufficient to trigger deep convection if the lifting is confined to too shallow of a layer or is of insufficient duration to allow air parcels to attain their LFC. PECAN?

- It is possible to use very high-resolution NWP models initialized with real data to study the structure and dynamics of bores important for convection initiation (see Koch et al. 2008). Successful real-time numerical prediction of bores and solitons depend upon whether the model can skillfully forecast:

  1. **Observed convective precipitation (typically the forcing for the density current and bore)**
  2. **The waveguide (e.g., frontal system, or inversion and LLJ depth/strength)**